

1 **Microbiota of the pregnant mouse: characterization of the bacterial communities in the**  
2 **oral cavity, lung, intestine, and vagina through culture and DNA sequencing**

3

4 **RUNNING TITLE: Pregnant mouse microbiota**

5 Jonathan M. Greenberg<sup>1,2</sup>, Roberto Romero<sup>1,3-6</sup>, Andrew D. Winters<sup>1,7,8</sup>, Jose Galaz<sup>1,2</sup>, Valeria  
6 Garcia-Flores<sup>1,2</sup>, Marcia Arenas-Hernandez<sup>1,2</sup>, Jonathan Panzer<sup>1,7</sup>, Zachary Shaffer<sup>1,8</sup>, David J.  
7 Kracht<sup>1,8</sup>, Nardhy Gomez-Lopez<sup>1,2,7\*</sup>, Kevin R. Theis<sup>1,2,7\*</sup>

8

9 **AUTHOR AFFILIATIONS**

10 <sup>1</sup> Perinatology Research Branch, Division of Obstetrics and Maternal-Fetal Medicine, Division  
11 of Intramural Research, *Eunice Kennedy Shriver* National Institute of Child Health and Human  
12 Development, National Institutes of Health, U.S. Department of Health and Human Services,  
13 Bethesda, MD, and Detroit, MI, United States

14 <sup>2</sup> Department of Obstetrics and Gynecology, Wayne State University School of Medicine,  
15 Detroit, MI, United States

16 <sup>3</sup> Department of Obstetrics and Gynecology, University of Michigan, Ann Arbor, MI, United  
17 States

18 <sup>4</sup> Department of Epidemiology and Biostatistics, Michigan State University, East Lansing, MI,  
19 United States

20 <sup>5</sup> Center for Molecular Medicine and Genetics, Wayne State University, Detroit, MI, United  
21 States

22 <sup>6</sup> Detroit Medical Center, Detroit, MI, United States

23 <sup>7</sup> Department of Biochemistry, Microbiology, and Immunology, Wayne State University School  
24 of Medicine, Detroit, MI, United States

25 <sup>8</sup> Department of Physiology, Wayne State University School of Medicine, Detroit, MI, United  
26 States

27

28 **CORRESPONDING AUTHOR(S)**

29 \* **Kevin R. Theis, [ktheis@med.wayne.edu](mailto:ktheis@med.wayne.edu)**

30 \* **Nardhy Gomez-Lopez, [ngomezlo@med.wayne.edu](mailto:ngomezlo@med.wayne.edu)**

31

32 **FUNDING SOURCES STATEMENT**

33 This research was supported, in part, by the Perinatology Research Branch (PRB), Division of  
34 Intramural Research, *Eunice Kennedy Shriver* National Institute of Child Health and Human  
35 Development, National Institutes of Health, U. S. Department of Health and Human Services  
36 (NICHD/NIH/DHHS), under Contract No. HHSN275201300006C. This research was also  
37 supported by the Wayne State University Perinatal Initiative in Maternal, Perinatal and Child  
38 Health (NG-L and KRT). The funders had no role in the study design, data collection and  
39 analysis, decision to publish, or preparation of the manuscript. Dr. Romero has contributed to  
40 this work as part of his official duties as an employee of the United States Federal Government.

41

42 **ABSTRACT**

43 Mice are frequently used as animal models for mechanistic studies of infection and obstetrical  
44 disease, yet characterization of the murine microbiota during pregnancy is lacking. The objective  
45 of this study was to therefore characterize the microbiotas of distinct body sites of the pregnant  
46 mouse that harbor microorganisms that could potentially invade the murine amniotic cavity  
47 leading to adverse pregnancy outcomes: vagina, oral cavity, intestine, and lung. The microbiotas  
48 of these body sites were characterized through anoxic, hypoxic, and oxic culture, as well as  
49 through 16S rRNA gene sequencing. With the exception of the vagina, the cultured microbiotas  
50 of each body site varied with atmosphere, with the greatest diversity in the cultured microbiota  
51 appearing under anoxic conditions. Only cultures of the vagina were able to recapitulate the  
52 microbiota observed from direct DNA sequencing of body site samples, primarily due to the  
53 dominance of two *Rodentibacter* strains. Identified as *R. pneumotropicus* and *R. heylii*, these  
54 isolates exhibited dominance patterns similar to those of *Lactobacillus crispatus* and *L. iners* in  
55 the human vagina. Whole genome sequencing of these *Rodentibacter* strains revealed shared  
56 genomic features, including the ability to degrade glycogen, an abundant polysaccharide in the  
57 vagina. In summary, we report body site specific microbiotas in the pregnant mouse with  
58 potential ecological parallels to those of humans. Importantly, our findings indicate that the  
59 vaginal microbiota of pregnant mice can be readily cultured, suggesting that mock vaginal  
60 microbiotas can be tractably generated and maintained for experimental manipulation in future  
61 mechanistic studies of host vaginal-microbiome interactions.

62

63

64

65 **IMPORTANCE**

66 Mice are widely utilized as animal models of obstetrical complications; however, the  
67 characterization of the murine microbiota has been neglected during pregnancy. Microorganisms  
68 from the vagina, oral cavity, intestine, and lung have been found in the intra-amniotic space,  
69 where their presence threatens the progression of gestation. Herein, we characterize the  
70 microbiotas of pregnant mice and establish the appropriateness of culture in capturing the  
71 microbiota at each site. The high relative abundance of *Rodentibacter* observed in the vagina is  
72 similar to that of *Lactobacillus* in humans, suggesting potential ecological parallels. Importantly,  
73 we report that the vaginal microbiota of the pregnant mouse can be readily cultured under  
74 hypoxic conditions, demonstrating that mock microbial communities can be utilized to test the  
75 potential ecological parallels between microbiotas in human and murine pregnancy, and to  
76 evaluate the relevance of the structure of these microbiotas for adverse pregnancy outcomes,  
77 especially intra-amniotic infection and spontaneous preterm birth.

78

79 **KEY WORDS:** **pregnancy, mouse model, microbiome, *Rodentibacter*, oral cavity, lung,**  
80 **intestine, vagina**

81

## 82 INTRODUCTION

83 Ethical and practical limitations on experimentation with humans are barriers to fully  
84 understanding the role of the microbiome in human health and disease. To overcome these  
85 limitations, researchers often perform experiments with *in vitro* cell culture models or *in vivo*  
86 animal models, presuming that these models accurately reflect host-microbiome dynamics in  
87 humans. In particular, the laboratory mouse is widely used for *in vivo* experimentation evaluating  
88 microbial causes of disease (1, 2). The mouse model has several benefits. First, of the available  
89 mammalian models, mice are relatively inexpensive to maintain and easy to manipulate  
90 experimentally. They can be housed in controlled environments, including environments that are  
91 germ-free, thereby reducing the impact of potential confounding variables on the microbiota and  
92 experimental outcomes related to health and disease. However, the mouse model is often used  
93 without consideration of the differences between the microbiotas of mice and humans or the  
94 potential differential impacts of the microbiota on health and disease in the two species (1, 3, 4).  
95 Specifically, experimental mouse studies often include the introduction of a human-specific  
96 microorganism into the mouse's microbiota or the transplantation of an entire body site-specific  
97 human microbiota into the mouse. A limitation of these studies is a lack of knowledge of a  
98 mouse's typical microbiota, making experimentally induced changes in the microbiota hard to  
99 interpret. This is further exacerbated by studies operating under the assumption that the human  
100 microbiota can be equivalently recreated within the mouse model or that interactions between the  
101 human microbiota and a mouse are the same as those between the human microbiota and a  
102 human (2). However, if parallels between the microbial ecology of human and mouse body site-  
103 specific microbiotas can be identified, and if mouse microbiotas can be tractably constituted  
104 through culture, manipulated in a targeted way, and reintroduced to the mouse, then focusing on

105 the mouse microbiota in investigations of mouse models of health and disease may be as or more  
106 fruitful than focusing on the human microbiota.

107 The intestinal microbiota of the mouse has been intensively studied and characterized (5-  
108 20). However, the microbiotas of the mouse oral cavity, lung, and vagina have received much  
109 less attention (**Supplemental Tables 1-3**), and only a select few studies have simultaneously  
110 characterized the microbiotas of multiple body sites in the mouse (5, 18, 21). This gap in  
111 knowledge is particularly apparent in studies of the mouse microbiota during pregnancy. The  
112 mouse has been widely used to investigate pregnancy complications, including perinatal  
113 infection and spontaneous preterm birth (22-38); yet, aside from the intestinal microbiota (15, 17,  
114 39), the microbiota of the mouse in the context of pregnancy has been largely overlooked (**Table**  
115 **1**). Given the widely reported associations between the human vaginal microbiota and pregnancy  
116 complications, such as intra-amniotic infection (40-43) and spontaneous preterm birth (36, 44-  
117 58), the baseline vaginal microbiota in the pregnant mouse should be thoroughly investigated and  
118 characterized. This is critical because the human vaginal microbiota is unique – humans are the  
119 only mammal known to have vaginal microbiotas that are often dominated by just a single  
120 bacterial species (i.e., one of four *Lactobacillus* spp.: principally *L. crispatus* or *L. iners*, and  
121 secondarily *L. gasseri* or *L. jensenii*) (59-61), and these microbiotas have been characterized into  
122 readily distinguishable vaginal community state types (CSTs) (62). These *Lactobacillus*-  
123 dominant CSTs (CSTs I-III, and V) are generally perceived as being conducive to reproductive  
124 health. Conversely, the relationship between human reproductive health and the non-  
125 *Lactobacillus*-dominant, and thus species rich and diverse, CST IV is more ambiguous (45, 55-  
126 57, 63-65). This disparity in health outcome potentially related to the structure of the vaginal  
127 microbiota is highlighted by the observation that women who do not have a *Lactobacillus*-

128 dominant vaginal microbiota prior to or during early pregnancy typically transition to a vaginal  
129 microbiota of *Lactobacillus*-dominance as gestation progresses (50, 51, 66), suggesting that  
130 pregnancy entails selective pressures for *Lactobacillus*-dominance in the vaginal  
131 microenvironment. Therefore, it is important to know if the vaginal microbiota of the mouse has  
132 similar or ecologically parallel characteristics to those of the human vagina microbiota given the  
133 propensity for the use of the mouse model in studies of pregnancy, intrauterine infection, and  
134 spontaneous preterm birth.

135 The microbiota of the oral cavity, lung, and intestine can also influence human pregnancy  
136 outcomes. Several studies have detected microorganisms from the oral cavity of pregnant  
137 women, especially *Fusobacterium nucleatum*, in the amniotic cavity, which is presumably due to  
138 hematogenous transfer and can result in stillbirth or spontaneous preterm birth (67, 68).  
139 *Mycoplasma pneumoniae* and *Mycobacterium tuberculosis*, bacteria known to colonize the  
140 human lung, have also been implicated in human intra-amniotic infection (69, 70). Additionally,  
141 *Streptococcus agalactiae* is a commensal bacterium in the human intestine and vagina, however,  
142 colonization of the neonate by this bacterium during delivery can cause adverse neonatal  
143 outcomes such as sepsis (71-73). Given the potential for pregnancy complications caused in part  
144 by microorganisms from the oral cavity, lung, intestine, and vagina in humans, understanding the  
145 structure of these murine microbiotas during gestation is required if the mouse is to be  
146 effectively used as a model for investigating the role of the microbiota in obstetrical  
147 complications.

148 The objectives of this study were therefore to characterize the microbiotas of the oral  
149 cavity, lung, intestine, and vagina of the pregnant mouse using anoxic, hypoxic and oxic culture,  
150 as well as 16S rRNA gene sequencing, and to compare and contrast the effectiveness of these

151 different microbiological approaches for characterizing the mouse microbiota (**Figure 1**). We  
152 found variation by atmosphere in the composition of microorganisms cultured, with a greater  
153 diversity of bacteria recovered under anoxic conditions. However, it was the profiles of bacterial  
154 communities cultured under hypoxic and oxic conditions that best matched the structure of the  
155 16S rRNA gene profiles of sampled body sites. Each body site had a unique microbiota; yet,  
156 multiple taxa were shared across body sites, suggesting a degree of interconnectedness among  
157 the microbiotas at these sites. Notably, potentially analogous to the human vaginal microbiota,  
158 the microbiota of the pregnant mouse vagina clustered into community state types (CSTs) based  
159 primarily on the dominance of two congeners, *Rodentibacter pneumotropicus* and *R. heylii*.  
160 Whole genome sequencing of cultured isolates of these two *Rodentibacter* species revealed  
161 genes associated with the utilization of glycogen, the predominant carbohydrate in the vagina.  
162 Importantly, the profiles of bacterial communities cultured from the vagina overlapped tightly  
163 with the 16S rRNA gene profiles of this body site. Therefore, culture can be used to accurately  
164 characterize the microbiota of the pregnant mouse vagina, and such can be successfully cultured  
165 and maintained in the laboratory and tractably manipulated for experimental *in vivo* studies of  
166 the vaginal microbiota and its role in pregnancy complications.

167

168 **RESULTS**

169 ***Influence of atmosphere and body site on the microbiota cultured from the oral cavity, lung,***  
170 ***intestine, and vagina***

171 *Alpha diversity*

172 Alpha diversity (i.e., the diversity within a single community) of the cultured microbiota varied  
173 by atmosphere (i.e., anoxic, hypoxic, oxic conditions) in all body sites except the vagina (**Figure**  
174 **2A-D**). In general, the cultured microbiota under anoxic conditions were more diverse than the  
175 cultured microbiota under hypoxic and oxic conditions; this observation was most pronounced  
176 for the cultured intestinal microbiota (**Figure 2C**). After bioinformatically pooling the cultured  
177 microbiota data from all atmospheres for each individual mouse by body site, variation in  
178 microbiota alpha diversity was clear among the four body sites (**Figure 2E**). The cultured  
179 intestinal microbiota was consistently the most diverse, while the cultured vaginal microbiota  
180 was consistently the least diverse (**Figure 2E**).

181 *Beta diversity*

182 Beta diversity (i.e., the diversity between two communities) of the cultured microbiota varied in  
183 composition and structure by both body site and atmosphere (**Table 2**, **Figure 3A-B**,  
184 **Supplemental Table 4-6**). Although atmosphere was a global driver of variation of the cultured  
185 microbiota, when the data for each body site were assessed separately by atmosphere  
186 (**Supplemental Figures 1-4**), variation in microbiota composition and structure was not  
187 observed for the lung or vagina (**Supplemental Table 5**; **Supplemental Figures 2 and 4**).  
188 Notably, mouse identity contributed to variation of the bacteria cultured from the vagina but not  
189 to that of the bacteria cultured from the three other body sites. Additionally, vaginal samples  
190 appeared to cluster into six distinct groups based on the most abundant cultured taxa

191 (Supplemental Figure 4C), suggesting the existence of vaginal community state types in the  
192 mouse. After bioinformatically pooling the culture data from all atmospheres by body site for  
193 each mouse, mouse identity and body site were identified as primary drivers of variation in the  
194 cultured microbiota (Figure 3), suggesting that the different atmospheres may have masked the  
195 influence of mouse identity in the previous analyses (Table 3).

196 ***Influence of atmosphere, controlled for body site, on the cultured microbiota***

197 *Oral cavity microbiota preferentially recovered under different atmospheres*

198 Under anoxic conditions, cultures of oral cavity microbiota appeared to cluster based on the  
199 relative abundance of either 1) *Lactobacillus* (Amplicon Sequence Variant 3 or ASV 3),  
200 *Muribacter muris* (ASV 4), and *Streptococcus* (ASV 32), or 2) *Rodentibacter* (ASV 2) and  
201 *Staphylococcus* (ASV 17) (Supplemental Figure 1C). This was contrasted with the cultures  
202 recovered under hypoxic and oxic conditions, which were consistently dominated by *Muribacter*  
203 *muris*, *Rodentibacter*, and *Staphylococcus* (Supplemental Figure 1C). Two LEfSe analyses  
204 were performed, one that was not restricted to a particular taxonomic classification level (i.e.,  
205 hierarchical analysis) and one that was restricted to the level of ASV. Hierarchical LEfSe  
206 analysis revealed preferential recovery of bacteria from the phylum Firmicutes under anoxic  
207 conditions, specifically of the genera *Enterococcus*, *Lactobacillus*, and *Streptococcus*  
208 (Supplemental Figure 1D), while members of the phyla Proteobacteria and Actinobacteria were  
209 preferentially recovered under oxic conditions, including the genera *Rodentibacter* and *Rothia*.  
210 Specific ASVs of each of these genera were identified in the ASV-level analysis (Supplemental  
211 Figure 5A) and included prominent ASVs 2, 3, 15, 79, from 4 of the genera identified in the  
212 hierarchical analysis (Supplemental Figure 1D).

213 *Intestinal microbiota preferentially recovered under different atmospheres*

214 The microbiota cultured from the intestine under anoxic conditions were characterized by high  
215 relative abundances of several *Bacteroides* and *Lactobacillus* ASVs, as well as low relative  
216 abundances of *Bifidobacterium* and *Parasutterella* ASVs (**Supplemental Figure 3C**).  
217 Hierarchical LEfSe analysis revealed a large number of taxa that were cultured preferentially  
218 under anoxic conditions compared to the other atmospheric conditions (**Supplemental Figure**  
219 **3D**). Notably, the phyla Bacteroidetes and Actinobacteria were heavily represented, as well as  
220 members of Firmicutes, especially Lachnospiraceae and Oscillospiraceae, and to a lesser extent  
221 members of the phyla “Desulfobacterota phyl. nov.” (74) (originally classified under the delta  
222 subdivision of Proteobacteria) and Verrucomicrobia. At the genus level, 13 genera were  
223 preferentially recovered in culture under anoxic conditions, including *Akkermansia*, *Bacteroides*,  
224 *Bifidobacterium*, *Colidextribacter*, Coriobacteriaceae UCG-002, *Desulfovibrio*, *Enterorhabdus*,  
225 *Faecalibaculum*, *Parasutterella*, *Lachnoclostridium*, Lachnospiraceae UCG-006, *Muribaculum*,  
226 and *Rikenella*. *Staphylococcus* was the only genus that was preferentially recovered under oxic  
227 conditions, and no genera were preferentially recovered under hypoxic conditions  
228 (**Supplemental Figure 3D**). The trends in the hierarchical analysis were consistent with those in  
229 the analysis restricted to the ASV-level. With respect to the intestine, 18 ASVs were  
230 preferentially recovered under anoxic conditions, including *Akkermansia muciniphila*, multiple  
231 *Bacteroides* ASVs, *Bifidobacterium*, *Lactobacillus*, and *Parasutterella* (**Supplemental Figure**  
232 **5C**). *Bacteroides* and *Lactobacillus* were also recovered in culture under hypoxic and oxic  
233 atmospheric conditions, but *Bifidobacterium* and *Parasutterella* were not (**Supplemental Figure**  
234 **3C**). *Rodentibacter* and *Staphylococcus* ASVs constituted a large proportion of the cultures  
235 obtained under hypoxic and oxic conditions, yet they were not recovered under anoxic conditions  
236 (**Supplemental Figure 3C**). The ASV-only analysis identified only one feature as discriminant

237 of oxic and hypoxic cultures, a *Staphylococcus* (ASV 17) and *Bacteroides acidifaciens* (ASV  
238 26), respectively (**Supplemental Figure 5C**).

239 *Lung and vaginal microbiota preferentially recovered under different atmospheres*

240 The profiles of microbiota cultured from the lung and vagina were not affected by atmosphere  
241 (**Supplemental Figures 2, 4**). However, LEfSe analysis identified *Streptococcus* (ASV 32) and  
242 *Bacteroides sartorii* (ASV 28) as being preferentially recovered under anoxic conditions from  
243 the lung (**Supplemental Figure 5B**). No taxa or ASVs were identified as being differentially  
244 recovered based on atmospheric conditions from the vagina.

245 *Influence of body site, controlled for atmosphere, on the cultured microbiota*

246 Between the four body sites, there were a total of 33 prominent ASVs (defined as having an  
247 average relative abundance  $\geq 1\%$  in at least one body site and atmosphere combination)  
248 (**Supplemental Figures 1C-4C**). Five ASVs were prominent among all four body sites  
249 (**Supplemental Table 7**). These five ASVs were classified as *Rodentibacter* (ASVs 2 and 5),  
250 *Lactobacillus* (ASV 3), *Staphylococcus* (ASV 17), and *Rothia nasimurium* (ASV 79). Twenty of  
251 the 33 ASVs were prominent in only one body site, typically either the intestine or lung, and  
252 limited to one or two samples at high relative abundance or multiple samples at a low relative  
253 abundance (**Supplemental Table 8**).

254 *Rodentibacter* was cultured from nearly all vaginal samples and at high relative  
255 abundance, yet the presence and abundance of the two *Rodentibacter* ASVs differed among  
256 vaginal samples. Specifically, in most mice, only one of the two *Rodentibacter* ASVs were  
257 abundant (**Supplemental Figure 4C**). In a minority of mice, both *Rodentibacter* ASVs were  
258 abundant. This contrasted with cultures from the other body sites, in which ASV 5 was much less

259 common and ASV 2 was limited to recovery under hypoxic or oxic conditions, except in a few  
260 oral samples (**Supplemental Figures 1C-4C**).

261 The prominent *Lactobacillus* (ASV 3) was cultured from most intestinal and lung  
262 samples regardless of atmosphere, exclusively under anoxic conditions from most of the oral  
263 samples and was highly abundant in only a single vaginal sample (the only vaginal sample  
264 without *Rodentibacter*). *Staphylococcus* (ASV 17) was commonly cultured from oral and  
265 intestinal samples but only rarely from lung samples. In the vagina, *Staphylococcus* (ASV 17)  
266 was exclusively cultured from samples that had an abundance of *Rodentibacter* ASV 5; it was  
267 only detected alongside *Rodentibacter* ASV 2 when ASV 5 was also abundant.

268 After bioinformatically pooling the culture data from each atmosphere by body site for  
269 each mouse, 21 ASVs were prominent in at least one body site (**Figure 3C**). Three ASVs were  
270 prominent among all four body sites, with the *Rodentibacter* ASVs 2 and 5 having the greatest  
271 average relative abundance in vaginal cultures (36.1% and 33.2%, respectively), and ASV 3  
272 (*Lactobacillus*) having the greatest average relative abundance in lung cultures (24.1%). Ten of  
273 these 21 ASVs were prominent in only one body site, with six being prominent only in intestinal  
274 cultures. Only one of the 21 prominent ASVs was exclusive to a single body site; ASV 106, an  
275 unclassified Actinobacteria, was unique to the lung.

276 LEfSe analysis revealed many taxa that were cultured preferentially from the intestine  
277 (**Figure 3D**). Specifically, members of the phyla Bacteroidetes and Firmicutes were  
278 preferentially recovered in the intestine (**Figure 3D**). At the genus level, 6 genera were  
279 preferentially recovered in cultures of the intestine, including *Bacteroides*, *Bifidobacterium*,  
280 Coriobacteriaceae UCG-002, *Faecalibaculum*, *Parasutterella*, and Lachnospiraceae UCG-006.  
281 Members of the Phylum Actinobacteria and genera *Escherichia/Shigella*, *Lactobacillus*,

282 *Muribacter*, and *Rothia* were preferentially recovered from the lung. *Enterococcus*,  
283 *Streptococcus*, and *Gemella* were preferentially recovered from the oral cavity, while  
284 *Rodentibacter* was preferentially recovered from the vagina (**Figure 3D**).

285 ***Cultured microbiota contrasted with molecular characterizations of the same samples***

286 Alpha diversity varied similarly for molecular profiles as was observed in the cultured  
287 microbiota. Variation was observed in both richness (Chao1, Friedman's test:  $F = 16.91$ ,  $p <$   
288 0.001) and evenness (Shannon and Inverse Simpson, Friedman's test:  $F = 16.91$ ,  $p < 0.001$ )  
289 between the oral cavity, intestine, and vagina. Pairwise comparisons revealed the intestine was  
290 more diverse than both the oral cavity (Wilcoxon singed rank tests for all three indices:  $W = 66$ ,  
291  $p < 0.001$ ) and vagina (Wilcoxon singed rank tests for all three indices:  $W = 66$ ,  $p < 0.001$ ),  
292 while the oral cavity and vagina were not (Wilcoxon singed rank test: Chao1,  $W = 18$ ,  $p = 0.206$ ;  
293 Shannon,  $W = 40$ ,  $p = 0.577$ ; Inverse Simpson,  $W = 31$ ,  $p = 0.898$ ). The low alpha diversities  
294 were largely due to high relative abundances of *Streptococcus danieliae* (ASV1) and  
295 *Rodentibacter* (ASV 2 and 5) observed in the oral cavity and vagina, respectively (**Figure 4A**).

296 In total, cultured surveys accounted for 411 ASVs contrasted with 751 ASVs in  
297 molecular surveys (**Supplemental Table 9**). Remarkably, only 339 ASVs were detected in both  
298 datasets, however both datasets had numerous ASVs not observed in the opposing dataset. For  
299 each body site, more ASVs were detected in molecular surveys than culture surveys except for  
300 the lung (**Supplemental Table 9**). Of the prominent ASVs among both datasets (ASVs with an  
301 average relative abundance  $\geq 1\%$  in at least one body site from culture or molecular samples),  
302 most ASVs were detected in both datasets overall, over 90% (46/51), and at least half were  
303 observed in both culture and molecular datasets at each body site (**Figures 4A**). Only 3 of the 39  
304 prominent molecular ASVs were not detected in culture surveys (**Figure 4B**). Two of these were

305 only prominent in the lung, while the third, ASV 22 was prominent in the lung and intestine, and  
306 was detected in the intestine of all 11 mice. Of the 21 ASVs prominent in the cultured bacterial  
307 profiles (**Figure 4A**), 11 were detected in all four body sites via molecular surveys while only  
308 two were not detected in any body site (ASV 106 and 123). Despite sharing a majority of  
309 prominent ASVs, correlations between culture and molecular profiles were only observed among  
310 the intestine and vagina (**Table 4**), likely due to the overlap of prominent ASVs and the  
311 dominance of *Rodentibacter* ASVs in the vagina.

312 ***Comparative genomics of the two predominant vaginal bacteria***

313 The distinct distribution and relative abundance patterns of ASV 2 and ASV 5 in the bacterial  
314 profiles of vaginal samples warranted further investigation of their genomic potential. ASV 2,  
315 identified as *Rodentibacter pneumotropicus* by 16S rRNA gene BLAST (75) analysis of  
316 sequenced isolates, and ASV 5, identified as *Rodentibacter heylii*, were submitted for whole  
317 genome sequencing to assess how the genomic and functional features of these two distinct  
318 *Rodentibacter* isolates might explain their distribution and abundance patterns in the murine  
319 vagina. The assembled genomes of both isolates were incorporated into a phylogenomic analysis  
320 of *Rodentibacter* type strains (**Figure 5A**), as well as all available *Rodentibacter* spp. genomes  
321 (**Figure 5B**). The genomes of the ASV 2 and ASV 5 isolates clustered as expected, based on the  
322 16S rRNA gene analysis, with the genomes of their conspecifics, and a summary of the general  
323 genomic features of the isolates and two additional strains is provided in **Supplemental Table**  
324 **10**.

325 Of the 2,384 genes present in the ASV 2 genome, 1,505 could be confidently assigned to  
326 a KEGG molecular network (76). The most represented categories were genetic information  
327 processing, environmental information processing, and carbohydrate metabolism (**Figure 5C**).

328 Analysis of complete pathways for carbohydrate degradation indicated that ASV 2 has the  
329 capacity to utilize glycogen and 12 sugars: 2-deoxy-alpha-D-ribose-1-phosphate, D-arabinose,  
330 fructose, fucose, galactose, glucose, D-mannose, melibiose, ribose, trehalose, xylose and nine-  
331 carbon keto sugars (sialic acids N-Acetylneuraminate and N-acetylmannosamine). The genomic  
332 potential of ASV 2 was compared to that of 16 other reported *Rodentibacter pneumotropicus*  
333 strains for which published genomes were available. The published strains contained 1,565 core  
334 genes that were also present in ASV 2. Based on Prokka annotation of genomes (77), the  
335 pangenome of the 17 strains consisted of 4,389 genes, with each strain containing an average of  
336 2,178 genes. Notably, ASV 2 contained the most genes (2,321) among these strains, followed by  
337 *R. pneumotropicus* strain Ac84 (2,311). Compared to the other *R. pneumotropicus* genomes, the  
338 genome of ASV 2 contained 83 unique genes, of which 81 are hypothetical proteins. The two  
339 unique genes with annotated functions were identified as DNA (cytosine-5-)methyltransferase  
340 (*ydiO*) and serine/threonine-protein phosphatase 1 (*pphA*). An additional 25 annotated genes  
341 were unique to ASV 2 and its most phylogenetically similar strain P441, including a secretory  
342 immunoglobulin A-binding protein (*esiB*), bifunctional polymyxin resistance protein (*arnA*), and  
343 lipooligosaccharide biosynthesis protein lex-1 (*lexI*).

344 For the *R. heylii* isolate ASV 5, 1,537 of 2,474 genes were confidently assigned to a  
345 KEGG molecular network (76), and as with ASV 2, genetic information processing,  
346 environmental information processing, and carbohydrate metabolism were the most represented  
347 categories (Figure 5). Complete pathways for carbohydrate degradation were very similar to  
348 those for ASV 2, including glycogen metabolism, with the exception that ASV 5 is not able to  
349 degrade 2-deoxy-alpha-D-ribose-1-phosphate, and it is able to degrade both L- and D- arabinose  
350 isomers, whereas ASV 2 can only utilize D-arabinose. The previously published genomes of 7 *R.*

351 *heylii* strains have a core genome of 1,649 genes, of which 1,644 were present in the genome of  
352 ASV 5. The 5 missing genes included two hypothetical proteins, Lipopolysaccharide export  
353 system permease protein LptG (*lptG*), a duplicate outer membrane protein A (*ompA*), and a  
354 duplicate Anthranilate synthase component 2 (*trpG*). Compared to the other *R. heylii* genomes,  
355 ASV 5 contained 182 unique genes, of which 155 were hypothetical proteins. Notable genes  
356 unique to ASV 5 include mRNA interferase toxin RelE (*relE*), a duplicate Lysozyme RrrD  
357 (*rrrD*), very short patch repair protein (*vsr*), Enterobactin exporter EntS (*entS*), a duplicate  
358 Endoribonuclease ToxN (*toxN*) found in only one other strain, and Colicin V secretion protein  
359 CvaA (*cvaA*). A unique feature of the genome of ASV 5 compared to those of other published *R.*  
360 *heylii* strains is the presence of genes from the lsr operon, which regulates the autoinducer-2  
361 quorum sensing pathway, suggesting that this strain may exhibit quorum-sensing, which may  
362 partially contribute to the distinct community structures observed in the present study.

363 Several differences in metabolic pathways were evident between the genomes of ASVs 2  
364 and 5. As facultative anaerobes, the genomes of ASVs 2 and 5 encode genes for fermentation;  
365 however, only ASV 2 has the necessary alcohol dehydrogenase gene, *adhE*, for metabolizing  
366 ethanol. Other features unique to ASV 2 include metabolism of nucleotide monophosphates, the  
367 amino acids alanine and proline, and the reduction of glutathione. Notably, ASV 2 is missing  
368 several enzymes involved in the TCA cycle including citrate synthase; conversely, ASV 5 is not.  
369 However, this observation was not unique to ASV 2, as these enzymes are also missing from the  
370 other published *R. pneumotropicus* genomes. Collectively, they encode for and use citrate lyase  
371 as an alternative route for citrate degradation. Pathway features that are present in ASV 5 and yet  
372 missing in ASV 2 include lysine decarboxylase (needed for the biosynthesis of cadaverine),  
373 prepilin peptidase (involved in pilus formation), nitrite reductase (involved in denitrification),

374 UDP-glucose:undecaprenyl-phosphate glucose-1-phosphate transferase (involved in colanic acid  
375 synthesis), and several enzymes necessary for the biosynthesis of the sialic acid CMP-N-  
376 acetylneuraminate. One interesting metabolic difference between the two ASVs is that ASV 5  
377 contains three genes for the degradation of glycogen whereas ASV 2 only contains one. Also,  
378 ASV 5 contains a suite of tight adherence protein genes (*tadB* and *tadD-G*) and several, but not  
379 all, genes necessary for operation of the type IV secretion system; *virB2* and *virB7* were not  
380 identified in the genome. Lastly, although the genomes of both isolates contain the gene  
381 encoding the LuxS protein (a metabolic protein also utilized in quorum sensing), only isolate  
382 ASV 5 carries the necessary downstream genes for quorum-sensing, suggesting a substantial  
383 ecological distinction between the two isolates.

384 Shared features of the genomes of both isolates involved in interacting with the  
385 extracellular environment include genes for the sec-SRP and tat export pathways, lap adhesins,  
386 type VI secretion system, and the metabolism of urea. Also, although the genome of ASV 2 does  
387 not have a putative prepilin peptidase gene, both isolates contain multiple genes involved in pilus  
388 formation. While both isolates share several notable functions associated with interacting and  
389 persisting in the environment, ASV 5 has a greater capacity to interact with the environment. The  
390 more robust genome of ASV 5 and the differences in metabolism warrant further exploration, as  
391 do the number of hypothetical proteins observed in the genomes of both species. Detailed  
392 experimental studies may elucidate the mechanisms underlying the distinct colonization patterns  
393 we observe in the mouse vagina, especially in the context of ASV 5's apparent unique quorum-  
394 sensing ability.

395

396 **DISCUSSION**

397 **Principal findings of the current study**

398 Preferential recovery of cultured microbiota was observed between anoxic, hypoxic, and oxic  
399 atmospheres with greater diversity of bacteria recovered under anaerobic conditions for each  
400 body site except for the vagina. Diversity of cultured microbiota varied by body site with the  
401 intestine having the greatest and the vagina having the lowest bacterial diversity. While some  
402 variation was evident between the cultured microbiota and molecular surveys for each body site,  
403 there was a strong positive correlation between the cultured microbiota and molecular profiles of  
404 the vagina. Bacterial profiles of the vagina were dominated by one or two distinct *Rodentibacter*  
405 strains (ASVs 2 and 5) using both culture and molecular approaches, indicating that the culture  
406 approaches employed herein accurately captured the vaginal microbiota. Whole genome  
407 sequencing of these *Rodentibacter* strains identified many shared genomic features, including the  
408 ability to metabolize glycogen, yet there were also strain-specific features, most notably a suite  
409 of quorum sensing genes exclusively observed in the ASV 5 strain.

410 **Impacts of atmosphere on the cultured microbiota of the mouse**

411 Bacteria are capable of growth and reproduction in a variety of atmospheric conditions but are  
412 often broadly categorized by their ability or lack thereof to utilize O<sub>2</sub> as a terminal electron  
413 acceptor during aerobic respiration under oxic conditions (78, 79). Notably, most of the body  
414 sites that are the focus of this study are typically low in O<sub>2</sub> concentration compared to ambient  
415 atmospheres and are thus often considered anaerobic environments (7). However, these sites  
416 exhibit an O<sub>2</sub> gradient, as O<sub>2</sub> diffuses out from the host tissues into the mucus layer and the  
417 tissue-microbiota interface (79). It has therefore been suggested that microbial culture at low  
418 level O<sub>2</sub> concentrations (i.e., hypoxic atmospheric conditions) will facilitate the growth of

419 bacteria present at this interface which are able to grow but are typically outcompeted by other  
420 bacteria at lower (anoxic) or higher (oxic) oxygen concentrations (i.e., the atmospheric  
421 conditions most frequently used for microbial culture) (79).

422 In the current study, anaerobic culture yielded the greatest diversity of bacteria for the  
423 intestine, lung, and oral cavity, but not for the vagina. This may suggest a bias of culturing  
424 anaerobic bacteria from the intestine, lung, and oral cavity or merely a greater capacity for  
425 anaerobic bacteria from these sites to grow under laboratory conditions. Regardless, the low  
426 degree of correlation between the culture and molecular profiles of the microbiotas in the oral  
427 cavity indicate that the culture methods used in this study were not sufficient for capturing the  
428 breadth of bacteria present in this body site. Notably, however, the cultured and molecular  
429 surveyed microbiotas of the vagina were largely congruent, especially when culture was  
430 performed under hypoxic conditions. This leads to two important conclusions. First, when  
431 culturing the vaginal microbiota of the pregnant mouse, culture under hypoxic conditions alone  
432 appears sufficient for capturing its members – oxic and anoxic cultures would only need to be  
433 performed if specific hypotheses about the microbiota and vaginal oxygen levels were being  
434 investigated. Second, the current study demonstrates that the vaginal microbiota of the pregnant  
435 mouse can be reliably captured through laboratory culture and thus it is feasible and tractable to  
436 generate culture libraries that can be used for *in vitro* and *in vivo* manipulative experimentation  
437 of the vaginal microbiota and/or intra-amniotic infection in murine animal models of pregnancy  
438 complications.

439 **Prior reports of the oral cavity, lung, and vaginal microbiotas of non-pregnant mice**

440 The microbiotas of body sites other than the intestine in laboratory mice have been only  
441 infrequently characterized by 16S rRNA gene sequencing. Studies characterizing the microbiotas

442 of the oral cavity, lung, or vagina of normal non-pregnant mice are identified and summarized in

443 **Supplemental Tables 1-3.**

444 Most studies characterizing the microbiota of the murine oral cavity have focused on a  
445 single mouse strain (i.e., C57BL/6) (**Supplemental Table 1**). The genera within the oral  
446 microbiota often differed between studies, suggesting that environment plays a large role in the  
447 composition of the oral microbiota. This was demonstrated explicitly when the oral microbiota of  
448 mice from different laboratories were compared (80). Of the relatively abundant genera in the  
449 oral cavity, *Lactobacillus*, *Staphylococcus*, and *Streptococcus* were observed in multiple studies  
450 (80-83). Notably, no studies have characterized the oral microbiota of mice using culture.

451 The microbiota of the murine lung has been characterized through several studies  
452 comparing the microbiota of diseased or treatment groups to that of control mice, as opposed to  
453 strictly descriptive studies of control or healthy mice (**Supplemental Table 2**). Little overlap of  
454 abundant genera has been observed among studies. In fact, one study acquired mice from two  
455 different breeding facilities, characterized the microbiota of the lung, and found that there were  
456 no core bacteria common to all mice and not a single bacterium was shared between the majority  
457 of mice (84). Yet, the authors did observe convergence of the lung microbiota of mice acquired  
458 from different facilities after a week of cohabitation, suggesting that the lung microbiota is  
459 dynamic and largely influenced by housing and social environments. Despite the pronounced  
460 role of the environment on the lung microbiota, several bacterial genera were relatively abundant  
461 in multiple studies: *Streptococcus*, *Lactobacillus*, *Pseudomonas*, and *Staphylococcus* (5, 84-87).  
462 Two studies of the lung microbiota have utilized culture alongside molecular approaches. In the  
463 first, only one bacterium was recovered, *Micrococcus luteus*, and only from culture (5). In the

464 second, *Stenotrophomonas* and *Ochrobactrum* were detected in both culture and molecular  
465 surveys of the lung (88).

466 Studies characterizing the vaginal microbiota of mice have also varied in the abundant  
467 genera observed, however, like the microbiotas of both the murine oral cavity and lung, members  
468 of *Lactobacillus*, *Staphylococcus*, and *Streptococcus* were observed in multiple studies  
469 (**Supplemental Table 3**). Two studies have each observed mice with similar vaginal microbiotas  
470 that could be clustered into at least two Community State Types (CSTs). In the first study,  
471 vaginal microbiota samples could be clustered into two CSTs based largely on the relative  
472 abundance of *Streptococcus* (>50% in one group and ≤ 10% in the other) (5). The second study  
473 included five vaginal CSTs which were defined by varying relative abundances of  
474 *Staphylococcus*, *Enterococcus*, *Lactobacillus*, and multiple lower abundance taxa (89). Although  
475 no study has characterized the vaginal microbiota in mice using both culture and molecular  
476 methods, two older studies did perform culture-based characterization of the vaginal microbiota  
477 in mice (90, 91). Both studies cultured members of *Streptococcus*, *Staphylococcus*, and  
478 *Lactobacillus*; one also consistently recovered *Corynebacterium* and *Actinomyces* (90), and the  
479 other recovered members of the Enterobacteriaceae and Bacteroidaceae families (91).

480 **Prior reports of the oral cavity, lung, intestinal, and vaginal microbiotas of pregnant mice**

481 Excluding our current and prior study (21), the data of which overlap, the mouse intestinal  
482 microbiota during pregnancy has been characterized six times, and the vaginal microbiota has  
483 been characterized twice (**Table 1**). Among the studies that characterized the intestinal  
484 microbiota of pregnant mice (**Table 1**), approximately 18 bacterial taxa were observed at high  
485 relative abundances. The following taxa were observed at high relative abundances in multiple

486 studies: S24-7, *Allobaculum*, *Bacteroides*, *Bifidobacterium*, *Candidatus Athromitus*,  
487 *Clostridiales*, *Lactobacillus*, and *Lachnospiraceae*.

488 The two prior studies which characterized the vaginal microbiota of pregnant mice also  
489 simultaneously characterized that of the intestine (92, 93). In the first study, researchers  
490 investigated the effect of stress on these microbiotas and subsequent downstream effects on the  
491 microbial colonization of newborn mice. 16S rRNA gene sequencing was performed on maternal  
492 fecal samples collected daily and on vaginal fluid collected on embryonic day 7.5 (92). The  
493 bacterial taxa that were relatively abundant in the fecal samples included *Sutterella*, *Prevotella*,  
494 S24-7, *Bacteroides*, *Odoribacter*, *Desulfovibrionaceae*, *Lachnospiraceae*, *Ruminococcaceae*, and  
495 *Oscillospira*. The alpha diversity of the maternal intestinal microbiota decreased early in  
496 pregnancy and the composition of the microbiota differed between early and late pregnancy. The  
497 vaginal microbiota of the pregnant control mice at 7.5 days gestation were mainly composed of  
498 *Clostridiales*, *Aggregatibacter*, *Lachnospiraceae*, *Prevotella*, *Helicobacter*, and S24-7.

499 In the second study, researchers evaluated the fetal compartments of mice for evidence of  
500 *in utero* bacterial colonization and characterized maternal intestinal and vaginal microbiotas to  
501 assess the source of any potential bacterial signals detected in the fetus (93). Samples from the  
502 maternal stool were relatively abundant in *Candidatus Arthromitus*, S24-7, and *Lactobacillus*,  
503 while the vaginal samples were predominantly composed of *Kurthia gibsonii*.

504 In the current study, similar to prior studies (**Table 1**), we observed high relative  
505 abundances of Muribaculaceae (i.e., S24-7), *Bacteroides*, *Bifidobacterium*, *Desulfovibrionaceae*,  
506 *Lactobacillus*, and *Lachnospiraceae* in the intestinal microbiota of the pregnant mouse (**Figure**  
507 **4**). Yet, our findings for the vaginal microbiota were distinct. We found the vaginal microbiota of  
508 pregnant mice to be dominated by *Rodentibacter*, *Helicobacter*, and *Lactobacillus* (**Figure 4**).

509 The differences between the microbiota observed by Jašarević et al. (92) and those described in  
510 current study could be due to the gestational age at time of sampling. In the former, samples of  
511 the vaginal microbiota were taken during early gestation, embryonic day 7.5 (E7.5) whereas in  
512 the present study they were taken at late gestation (E17.5), which may suggest a shift in the  
513 vaginal microbiota that occurs between early and late gestation. In Younge et al. (93), vaginal  
514 samples were collected at one of three timepoints (E14-16, E17-18, E19-20) between mid to late  
515 gestation, however only two mice were sampled per group. The vaginal microbiota of the earlier  
516 timepoint consisted primarily of *Candidatus Arthromitus* and S24-7, which was similar to what  
517 was observed in the stool samples from those same mice. At the latter two timepoints, the  
518 vaginal microbiota were distinct from maternal stool with low diversity and high relative  
519 abundance of *Kurthia gibsonii*. Although no *Kurthia* sequences were detected in the current  
520 study, the low diversity observed in both studies suggests that the murine vaginal  
521 microenvironment changes during pregnancy and is permissive to the dominance of certain  
522 bacteria in the vagina.

### 523 **Bacterial Community State Types (CSTs) of the mouse vagina**

524 In a previous study, five Community State Types (CSTs) were suggested for the non-pregnant  
525 mouse vagina (89). The authors described these as being dominated by *Staphylococcus* and/or  
526 *Enterococcus*, *Lactobacillus*, or a mixed population of bacteria. While these bacteria were also  
527 detected in our study of pregnant mice, aside from *Lactobacillus*, they were not observed at high  
528 relative abundances, suggesting a potential shift in the vaginal microbiota of non-pregnant mice  
529 upon becoming pregnant. In our study, we almost exclusively observed a vaginal microbiota  
530 dominated by one or two distinct *Rodentibacter* strains that were widespread among the mice.  
531 These dominant strains/ASVs potentially mirror the dominance of *Lactobacillus crispatus* and *L.*

532 *inners* in prominent CSTs of the human vagina (62), suggesting the vagina of the pregnant mouse  
533 may represent a similar but unique ecological niche conducive to the proliferation of only a few  
534 dominant bacteria. This is especially interesting considering that during human pregnancy the  
535 vaginal microbiota typically shifts even more dramatically to a *Lactobacillus*-dominant  
536 community, especially later in gestation, and for those women who had non-*Lactobacillus*-  
537 dominant communities before pregnancy (66).

### 538 **Novel insights into *Rodentibacter* strains in the pregnant mouse vagina**

539 The assembled genomes for cultured isolates of *Rodentibacter* ASVs 2 and 5 are representative  
540 of *R. pneumotropicus* and *R. heylii*, respectively (Figure 5). It is unclear if these strains are  
541 uniquely adapted to murine vaginal microenvironments in general, or if this phenomenon is  
542 limited to pregnant mice, or even potentially pregnant mice in the specific animal housing  
543 facility under investigation here. Notably, this may be a general phenomenon as Jasarevic et al.  
544 (94) recently found *Pasteurella pneumotropica* to be abundant in the vagina of mice after  
545 pregnancy. In 2017, *P. pneumotropica* was reclassified to the genus *Rodentibacter* (94),  
546 indicating that this observation of *Rodentibacter* dominance is not exclusive to our animal  
547 facility.

548 The functional potential of both species suggests a wide range of metabolic capabilities  
549 like the ability to process various sugar sources, which may partially explain why both isolates  
550 were detected in multiple body sites of the mouse. Additionally, the genomes of both isolates  
551 indicate these strains can utilize glycogen which is a primary carbon source in the vagina (95).  
552 The larger genome size of ASV 5 and the greater number genes encoding of glycogen  
553 degradation enzymes may provide a more robust capacity to colonize and persist in the vaginal

554 microenvironment and may partially explain why other ASVs co-occurred less frequently in  
555 ASV 5-dominant vaginal samples than in ASV 2-dominant samples.

556 The relationship of these two *Rodentibacter* isolates and their murine host appears highly  
557 similar to the relationship between *Lactobacillus crispatus* and *L. iners* and their human host.  
558 First, members of both genera are capable of inhabiting multiple body sites of their hosts (96-  
559 101). Second, the highest relative abundance among the populated body sites in both hosts is  
560 within the vagina, wherein relative abundances can exceed 90% of the sequenced microbiota (50,  
561 59, 62, 66). Third, both isolates have the genomic capacity to degrade glycogen, which is a  
562 predominant carbon source in the mammalian vagina and is associated with the abundance of  
563 *Lactobacillus* in the human vagina (60, 102). Although *Rodentibacter* dominance in the pregnant  
564 mouse vagina has not been previously documented, this microbiota has been understudied  
565 (**Table 1**). It is possible that a low diversity microbiota dominated by *Rodentibacter* is evidence  
566 of a shift in vaginal microbiota structure during pregnancy in the mouse. In humans,  
567 *Lactobacillus*-dominance during normal pregnancy is common and associated with healthy term  
568 gestations, whereas more diverse vaginal microbiotas are less common among pregnant women  
569 and have been associated with adverse pregnancy outcomes (60, 66). The *Rodentibacter*-  
570 dominant vaginal microbiotas observed in this study may represent a similar transition in mice.  
571 Specifically, the vaginal microbiotas of mice may be typically more diverse, akin to CST IV in  
572 the human vagina, and transition to a less diverse, *Rodentibacter*-dominant state during  
573 pregnancy. This needs to be investigated further.

574 **Strengths of this study**

575 This was the first study to simultaneously characterize the microbiota of the oral cavity, lung,  
576 intestine, and vagina of the pregnant mouse through both culture and 16S rRNA gene sequence-

577 based approaches. It was also the first study to consider the extent to which culturing the  
578 microbiota from these body sites under different atmospheric conditions captured the complete  
579 site-specific microbiota, as defined through the molecular surveys. This study revealed strong  
580 associations of *Rodentibacter* strains with the vagina of the pregnant mouse, and whole genome  
581 sequencing of cultured representatives of these strains identified functional features that may  
582 explain their dominance with the murine vagina during pregnancy.

### 583 **Limitations of this study**

584 This study focused on C57BL/6 late-gestation pregnant mice from a single facility. This is  
585 important because there can be variation in the microbiota of mice across facilities (103, 104), as  
586 well as in the same laboratories over time (19). Therefore, it is not yet clear the extent to which  
587 the patterns in body-site specific microbiota data reported herein can be extrapolated to other  
588 studies. Additionally, non-pregnant mice and samples from pregnant mice at different gestational  
589 ages were not included and therefore the relationship of the microbiota throughout gestation  
590 could not be assessed. Nevertheless, this study provides a detailed foundational knowledge,  
591 based on multi-atmospheric culture and DNA-based sequencing approaches, of the microbiotas  
592 of the oral cavity, lung, intestine, and vagina of the pregnant mouse, thereby setting the stage for  
593 additional investigations into the reproductive microbial ecology of the mouse.

### 594 **Conclusions**

595 The microbiota of the pregnant mouse includes bacteria shared among the oral cavity, lung,  
596 intestine, and vagina. Yet, variation was evident in the microbiotas across body sites.  
597 Comparisons of culture and molecular microbiota profiles indicate that culture, especially  
598 hypoxic culture, effectively captured the microbiota of the vagina, but not necessarily of the  
599 other body sites. As the vaginal microbiota can be effectively cultured, moving forward it can be

600 tractably used for *in vitro* and *in vivo* experimentation evaluating relationships between the  
601 vaginal microbiota and adverse pregnancy outcomes in mice. The vaginal microbiota of the  
602 pregnant mouse appears to be dominated by one or two *Rodentibacter* strains, similar to the two  
603 *Lactobacillus*-dominant CSTs (i.e., I and III) in the human vagina during pregnancy. Whole  
604 genome sequencing of the *Rodentibacter* strains dominating the pregnant mouse vaginal  
605 microbiota here revealed the capacity to metabolize glycogen, a principal carbon source in the  
606 mammalian vagina. This capacity is also possessed by human vaginal lactobacilli. These findings  
607 suggest the existence of ecological parallels between the vaginal microbiotas of mice and  
608 humans during pregnancy. These parallels and their relevance to host reproduction warrant  
609 further investigation.

610 **MATERIALS AND METHODS**

611 ***Study subjects and sample collection***

612 Culture and DNA sequencing surveys of samples from the oral cavity, lung, intestine, and vagina  
613 of 11 pregnant mice that were included in our previous study evaluating the *in utero* colonization  
614 hypothesis (21) were here analyzed in-depth in effort to characterize and compare the  
615 composition and structure of the pregnant mouse microbiota across body sites (Figure 1). This  
616 study includes previously unpublished information on the culture of microorganisms from these  
617 body sites across atmospheric and growth media conditions, as well as functional genomic  
618 information on the principal *Rodentibacter* species inhabiting the murine vagina. Animal  
619 procedures were approved by the Institutional Animal Care and Use Committee at Wayne State  
620 University (protocol 18-03-0584).

621 ***Bacterial culture***

622 Bacterial culture was performed on intestinal and lung tissues and oral and vaginal swabs under  
623 oxic, hypoxic (5% O<sub>2</sub>, 5% CO<sub>2</sub>), and anoxic (5% CO<sub>2</sub>, 10% H, 85% N) conditions at 37°C for  
624 seven days. Under each atmosphere, samples were plated in duplicate onto tryptic soy agar with  
625 5% sheep's blood and chocolate agar. Samples were also plated on MacConkey agar under oxic  
626 conditions. If bacterial growth was observed (most typically a lawn of bacteria or too many  
627 colonies to count), the bacteria were collected by pipetting 1-2 ml of sterile PBS solution onto  
628 the agar plate and dislodging colonies with sterile and disposable spreaders and loops. These  
629 plate wash solutions (105) were stored at -80°C until DNA extractions were performed. DNA  
630 extractions were completed using a Qiagen DNeasy PowerSoil (Germantown, MD) extraction  
631 kit, as previously described (21). The V4 region of the 16S rRNA gene copies in DNA  
632 extractions were targeted using protocols previously described in Kozich et al. (106), and

633 sequenced on an Illumina MiSeq system at Wayne State University, as previously described in  
634 Theis et al. (21). Ultimately, 16S rRNA gene sequence libraries were generated for the cultures  
635 from 117/ 132 (89%) murine body site samples.

636 ***DNA sequencing surveys***

637 Tissue samples of the lung, distal intestine, and proximal intestine were collected in addition to  
638 swabs of the oral cavity and vagina and stored at -80°C until DNA extractions were performed.  
639 DNA extractions of samples for molecular surveys were performed in a biological safety cabinet  
640 by study personnel donning sterile surgical gowns, masks, full hoods, and powder-free exam  
641 gloves. Extracted tissue masses ranged from 0.016 to 0.107 g, 0.053 to 0.097 g, and 0.034 to  
642 0.138 g for the lung, distal intestine, and proximal intestine, respectively. Two types of negative  
643 technical controls were included in the DNA extraction and sequencing processes to address  
644 potential background DNA contamination: 1) sterile swabs as a negative control for body sites  
645 sampled with a swab (i.e., oral and vaginal sites), and 2) extraction tubes with no biological input  
646 as a negative control for body sites from which tissue was collected (i.e., proximal intestine,  
647 distal intestine, and lung).

648 DNA was extracted from tissues, swabs, and technical controls (i.e., swabs [n = 11] and  
649 blank DNA extraction kits [n = 23]) using the Qiagen DNeasy PowerLyzer PowerSoil kit with  
650 minor modifications to the manufacturer's protocol. Specifically, samples were added to the  
651 supplied bead tube along with 400 µl of bead solution, 200 µl of phenol-chloroform-isoamyl  
652 alcohol (pH 7 to 8), and 60 µl of solution C1. Mechanical lysis of cells was done using a bead  
653 beater for 30 seconds. Following centrifugation, the supernatants were transferred to new tubes  
654 and 100 µl of solutions C2 and C3 in addition to 1 µl of RNase A enzyme were added and tubes  
655 were incubated for 5 minutes at 4°C. After centrifugation, supernatants were transferred to new

656 tubes containing 650  $\mu$ l of solution C4 and 650  $\mu$ l of 100% ethanol prior to adding to the filter  
657 column, and 60  $\mu$ l of solution C6 for elution. The lysates were loaded onto filter columns until  
658 all sample lysates were spun through the filter columns. Five hundred microliters of solution C5  
659 was added to the filter columns and centrifuged for 1 minute, the flowthrough was discarded, and  
660 the tube was centrifuged for an additional 3 min as a dry spin. Finally, 100  $\mu$ l of solution C6 was  
661 placed on the filter column and incubated for 5 min before centrifuging for 30s to elute the  
662 extracted DNA. Purified DNA was stored at -20°C until 16S rRNA gene sequencing.  
663 Amplification and sequencing of the V4 region of the 16S rRNA gene were performed at the  
664 University of Michigan's Center for Microbial Systems as previously described (21), with library  
665 builds performed in triplicate and pooled for each individual sample prior to the equimolar  
666 pooling of all sample libraries for multiplex sequencing.

667 ***16S rRNA gene sequence processing of bacterial culture and molecular samples***

668 Raw sequence reads were processed using the DADA2 package in R following the tutorial  
669 pipeline as described by Callahan et al. (107) with minor modifications. Specifically, length of  
670 the reverse read truncation length was increased from 160 to 200 (“truncLen=c(240,200”)), the  
671 maximum expected errors in reverse reads was increased from 2 to 7 (“maxEE=c(2,7”)), and for  
672 sample inference samples were pooled to increase sensitivity (“pool=TRUE”). Sequences were  
673 ultimately classified into amplicon sequence variants (ASVs) and taxonomically identified using  
674 the Silva rRNA database v 138.1 (108, 109). After processing 16S rRNA gene sequences  
675 through DADA2, any ASVs identified as mitochondria, chloroplasts, and those not assigned to a  
676 bacterial phylum were removed.

677 Following DADA2 processing and removal of non-bacterial 16S rRNA gene sequences,  
678 only samples with libraries of at least 100 quality-filtered sequences were analyzed. From the

679 culture samples two samples fell below this threshold and were removed from subsequent  
680 analyses (1 anoxic mid-intestine sample and 1 hypoxic lung sample). For the molecular samples,  
681 all vaginal, oral cavity, proximal intestine, and distal intestine sequence libraries met this  
682 criterion, but only five lung libraries remained. The full dataset included 176 biological samples,  
683 15 blank extraction kit controls, and 17 negative swab controls representing a total of 1138  
684 ASVs.

685 To validate that the bacterial signals detected in the molecular surveys of mouse samples  
686 were legitimate, the composition and structure of the bacterial profiles of tissues and swabs were  
687 contrasted with those of blank ( $n = 15$ ) and blank swab ( $n = 17$ ) technical controls using the  
688 adonis function in the *vegan* package. For each body site, the composition and structure of  
689 bacterial profiles were distinct from those of applicable negative controls (**Supplementary**  
690 **Table 11**).

691 *Removal of background DNA contaminant ASVs through decontam*

692 After establishing that the 16S rRNA gene profiles of the tissue and swab samples from the  
693 pregnant mice were distinct from those of negative controls, the tissue and swab datasets were  
694 separately analyzed with *decontam* (110) to identify ASVs that were likely background DNA  
695 contaminants. Histogram plots of the distribution of prevalence scores indicated a threshold of  
696 0.8 would be appropriate for both datasets, thereby retaining a large percentage of ASVs (82% in  
697 the tissue dataset and 72% in the swab dataset). Between the two datasets, 209 ASVs were below  
698 the 0.8 threshold and identified as contaminants. 24 ASVs were not detected in any biological  
699 samples from the molecular surveys and 179 ASVs had an average relative abundance below 1%  
700 for each of the biological sample types. Three of the remaining 6 ASVs, *Ralstonia* (ASV 76),  
701 *Streptococcus* (ASV 520), and a *Bacillus* (ASV 6), were detected as contaminants in both tissue

702 and swab datasets. *Streptococcus* (ASV 11), *Muribacter* (ASV 4), and *Rodentibacter* (ASV 5),  
703 the 3 remaining ASVs, had average relative abundances above 1% in at least one body site from  
704 the opposing sample type (e.g., ASV 5 was above 1% average relative abundance in vaginal  
705 swabs but identified as a contaminant by *decontam* from the tissue dataset) suggesting that they  
706 may be legitimate sequences and were not considered contaminants and were retained in  
707 subsequent analyses. To allow for comparisons of the molecular datasets with the culture  
708 datasets, the *decontam* results were contrasted with the culture data to ensure that ASVs  
709 abundant in culture surveys were not removed as contaminants due to the fact that they were  
710 recovered via culture (i.e., they were legitimate as they were cultured by us). ASVs classified as  
711 contaminants through *decontam* were retained in subsequent analyses if they either were above  
712 1% average relative abundance in at least one cultured body site or cultured from at least 5 mice  
713 for a given body site. Thirteen additional ASVs met these criteria and ultimately 16 out of the  
714 209 ASVs identified as potential contaminants by *decontam* were kept in the datasets for  
715 subsequent analyses.

716 To aid comparisons of culture and molecular datasets, the molecular 16S rRNA gene  
717 profiles of the proximal and distal portions of the intestine were assessed for differences in their  
718 bacterial profiles using the adonis function in *vegan*. No differences were observed for either  
719 composition (mouse identity,  $p = 0.19$ ; intestine locale,  $p = 0.47$ ) or structure (mouse identity,  $p$   
720 = 0.14; intestine locale,  $p = 0.26$ ), and these samples were bioinformatically pooled by mouse  
721 identity and considered “intestinal” samples from molecular surveys. These data were contrasted  
722 with those of cultures from the mid-intestine.

723 ***Whole genome sequencing and genomic analysis of isolates ASV 2 and ASV 5***

724 *DNA extraction from bacterial isolates*

725 The 16S rRNA gene sequences associated with ASV 2 and ASV 5 were queried against a  
726 BLAST database of 16S rRNA gene sequences from isolates recovered and preserved during the  
727 previous study (21). Isolates with a 100% match were recovered from frozen stocks by plating 80  
728  $\mu$ l onto the media and atmosphere they were originally recovered on (both isolates were  
729 recovered on chocolate agar plates and under hypoxic atmospheric conditions (5% O<sub>2</sub>, 5% CO<sub>2</sub>,  
730 90% N<sub>2</sub>) and incubated for 48 hours. Colonies were then collected using sterile inoculating loops  
731 into 500  $\mu$ l of sterile PBS and centrifuged at 15,000 x g for 10 minutes. DNA extractions were  
732 performed using a DNeasy PowerLyzer PowerSoil Kit (QIAGEN, Valencia, CA, USA) and the  
733 first step included resuspension of the pelleted colonies in 500  $\mu$ l of bead solution and adding the  
734 total resuspended volume to the bead tubes. Two additional modifications to the manufacturer's  
735 protocol were made: (1) 100  $\mu$ l of solutions C2 and C3 were combined into a single step  
736 followed by 5-minute incubation at 4°C and subsequent centrifugation; (2) In the final elution  
737 step, DNA was eluted with 60  $\mu$ l of solution C6 rather than 100  $\mu$ l to increase DNA  
738 concentration. Extracted DNA was then stored at 4°C until submission (< 48 hours) for whole  
739 genome sequencing (WGS).

740 *Construction and sequencing of sample DNA libraries*

741 Libraries were built using the Illumina DNA Prep protocol and Nextera DNA CD indexes  
742 (Illumina). Libraries were sequenced at the Perinatology Research Branch using iSeq 100  
743 reagents (Illumina) with the iSeq 100 system (Illumina) and an output of 2 x 150 bp paired-end  
744 reads.

745 *DNA sequence processing and genome assembly*

746 Adapters from the raw sequence reads were removed using Trimmomatic (v0.35). Genome  
747 assembly was performed using SPAdes (v 3.12.0) through the web-based Galaxy platform (111)

748 with default parameters, except that k-mer sizes of 27, 37, 47, 57, 67, 77, and 87 were used.  
749 Contigs of less than 200 bp were removed after assembly and the average coverage per contig  
750 was 429 for ASV 2 and 256 for ASV 5.

751 *Phylogenomic analysis of ASV 2 and ASV 5 isolates in the context of other Rodentibacter*  
752 *genomes*

753 Phylogenomic analysis was performed using the up-to-date bacterial core gene (UBCG) tool  
754 (112) for phylogenomic tree inference, which utilized 92 core genes to assess phylogenomic  
755 relationships. The assembled genomes for isolates of ASV 2 and ASV 5, along with published  
756 *Rodentibacter* type strain genomes (downloaded through NCBI GenBank's ftp server), and  
757 secondarily with all published *Rodentibacter* genomes, were processed through the UBCG  
758 pipeline using default parameters in Virtualbox. For the phylogenomic tree featuring only  
759 published type strains, *Muribaculum intestinalis* was included as an outgroup and *Muribacter*  
760 *muris* was included as a within-family (Pasteurellaceae) outgroup. Trees were rooted on the  
761 midpoint using FigTree (v1.4.4) (113).

762 *Genome annotation and analysis of ASV 2 and ASV 5 isolates*

763 Prior to genome annotation, the contigs for each assembled genome were reordered and aligned  
764 to their closest strain, *R. pneumotropicus* strain P441 and *R. heylii* strain G1 for isolates ASV 2  
765 and ASV 5, respectively, using Mauve multiple genome alignment software (v 20150226) (114).  
766 The 16 published genomes of *R. pneumotropicus* along with isolate ASV 2 were annotated with  
767 Prokka (v 1.14.5) (77) and processed through Roary (v 3.13.0) (115) to establish a core genome  
768 for *R. pneumotropicus* and to subsequently assess the representation of this core genome in the  
769 genome of isolate ASV 2. This process was repeated for isolate ASV 5 and the 7 published  
770 genomes of *R. heylii*. Prokka and Roary tools were run through Galaxy with default parameters

771 except that paralog genes were not split when using Roary. For functional and pathway analysis,  
772 the genomes of isolates ASV 2 and ASV 5 were annotated with NCBI's Prokaryotic Genome  
773 Annotation Pipeline (PGAP) (116) tool using default parameters. These annotated genomes were  
774 submitted to the KEGG Automatic Annotation Server (KAAS) (117) for KEGG pathway  
775 enrichment analysis using only bacteria included in the representative set of "Prokaryotes" as the  
776 template data set for KO assignment and a bi-directional best hit assignment method. For  
777 detailed metabolic comparisons of complete pathways, Pathway/Genome databases (PGDBs)  
778 were generated using the assembled genomes for isolates ASV 2 and ASV 5 with Pathway Tools  
779 software (v 25.0) (118). Default parameters were used; however, several manual refinement  
780 steps were required per the User's Guide, including assigning probable enzymes, modified  
781 proteins, predicting transcription units, and inference of probable transporters.

782 ***Statistical analysis***

783 ***Alpha diversity***

784 The alpha diversities of bacterial culture profiles for each body site under each atmosphere were  
785 characterized by the Chao1 (richness), Shannon (evenness), and Inverse Simpson (evenness)  
786 indices and variation in diversity was assessed for culture profiles under each atmosphere  
787 separately for each body site. Then after bioinformatically pooling mice that had culture profiles  
788 from three atmospheres for all four body sites ( $n = 5$ ), diversity was compared between body  
789 sites. When comparing all three atmosphere culture profiles, datasets for each body site were  
790 rarefied to their lowest read depths (oral cavity: 3976 reads, lung: 358 reads, intestine: 4745  
791 reads, vagina: 7719 reads). When comparing diversity between body sites, each individual  
792 mouse's pooled samples were rarefied to the lowest read depth (20,954 reads). Alpha diversities  
793 of sequenced microbiota (molecular profiles) of the oral cavity, intestine, and vagina were also

794 compared in the same way and rarefied to the lowest read depth (810 reads); the lung was  
795 excluded from this analysis due to low sample size (n = 4). Rarefaction was performed in R with  
796 the *phyloseq* package. Alpha diversities were calculated and visualized in R using the *phyloseq*  
797 package and labeled in Adobe Illustrator. Alpha diversities were statistically evaluated with the  
798 *rstatix* package in R by repeated measures ANOVA or Friedman's ANOVA followed by paired  
799 t-tests or Wilcoxon signed rank tests when appropriate.

800 *Beta diversity*

801 Statistical comparisons of beta diversities were performed using the *vegan* and *pairwiseAdonis2*  
802 packages in RStudio (v 1.3.1093) and R (v. 4.0.3). Non-parametric multivariate analysis of  
803 variance (NPMANOVA) tests were used to evaluate the composition and structure of bacterial  
804 profiles using the Jaccard and Bray-Curtis Dissimilarity Indices, respectively. For comparisons  
805 where variation by mouse identity was observed, it was secondarily controlled for using the  
806 "strata" term on mouse identity in adonis and pairwise.adonis2 functions in *vegan* and  
807 *pairwiseAdonis2* packages, respectively. The composition and structure of bacterial profiles were  
808 visualized with Principal Coordinates Analysis (PCoA) plots generated using the RAM package  
809 in R (v. 4.0.3).

810 *Linear discriminant analysis Effect Size (LEfSe)*

811 LEfSe analyses were performed to identify features, taxa (assessed as hierarchical analyses), or  
812 ASVs (assessed as ASV-only analyses) that were preferentially recovered in different  
813 atmospheres for each body site and secondarily in each body site after bioinformatically pooling  
814 culture data from each atmosphere. To identify taxa that were differentially abundant in the  
815 hierarchical analysis, each taxonomic level from phylum to species was included for each  
816 individual ASV, when available. In assessing bacterial profile features preferentially recovered

817 in one atmosphere over the other two, or in one body site over the other three, only mice with  
818 cultures from all three atmospheres in a body site were included (n = 9 for oral cavity, intestine,  
819 and vagina; n = 7 for the lung).

820 For all LEfSe analyses, singleton features were removed from each dataset, multi-class  
821 analysis of all-against-all was used only in identifying features that were preferentially abundant  
822 in one condition over all the others, and only features with an LDA score above 3.0 were  
823 considered preferentially abundant. Histograms (ASV-only analyses) and cladograms  
824 (hierarchical analyses) were generated using the Galaxy hub. Each taxon is indicated on  
825 cladograms when identified as a significant feature except order (to avoid visual congestion).

826 *Mantel tests*

827 Mantel tests were used to determine whether there was a correlation between the structure of  
828 bacterial culture profiles and the structure of molecular profiles for each body site. Only mice  
829 with bacterial profiles in both culture and molecular datasets in a body site were evaluated.  
830 Mantel tests were performed on Bray-Curtis distance matrices using the *vegan* package in  
831 RStudio (v 1.3.1093) and R (v. 4.0.3).

832 *Figures*

833 Heatmaps were generated using gplots and Heatplus packages in R (v. 4.0.3) and clustering of  
834 samples was performed on Bray-Curtis dissimilarity distance matrices using an unweighted pair  
835 group method with arithmetic mean (UPGMA) in the hclust function in R.

836 *Data availability*

837 Original sample-specific MiSeq run files are available in the Short Read Archive from the  
838 original study Theis et al. (21), (BioProject identifier [ID] PRJNA594727). Assembled genomes

839 of isolates ASV 2 and ASV 5 with annotations from NCBI's Prokaryotic Genome Annotation

840 Pipeline are available at BioProject ID PRJNA823350.

841

842

843 **TABLES**

844 **Table 1. Description of previous 16S rRNA gene studies of the pregnant mouse**  
845 **microbiome.**

Author	Year	Body site	Microbiota culture methods	Mouse strain	Key microbiota findings
Gohir, et al. (119)	2015	Intestine	Not performed	C57BL/6J	<i>Akkermansia, Clostridium, Bacteroides, and Bifidobacterium</i> were increased in pregnant control mice compared to non-pregnant mice. Other abundant taxa observed in pregnant mice included <i>Lactobacillus, Alistipes, and Lachnospiraceae</i> .
Jašarević, et al. (92)	2017	Intestine, vagina	Not performed	C57BL/6:1 29	Relatively abundant taxa in the intestine included S24-7, <i>Prevotella</i> , an unclassified Clostridiales, and <i>Sutterella</i> . In the vagina, the top mean relative abundant taxa were <i>Aggregatibacter, Lachnospiraceae, and Clostridiales</i> at embryonic day 7.5.
Nuriel-Ohayon, et al. (120)	2019	Intestine	Not performed	Swiss Webster	Most abundant taxa included S24-7, Clostridiales, Rikenellaceae, Bifidobacteria, Lachnospiraceae, <i>Lactobacillus</i> , and <i>Turicibacter</i> .
Younge, et al. (93)	2019	Intestine, vagina	Not performed	C57BL/6	Most abundant taxa in the stool included S24-7, <i>Candidatus Athromitus</i> , and <i>Allobaculum</i> , while the vagina was largely dominated by <i>Kurthia</i> .
Faas, et al. (39)	2020	Intestine	Not performed	C57BL/6J OlaHsd	The intestinal microbiota at gestational days 7 and 14 were similar to the microbiota before pregnancy, however at gestational day 18, the microbiota became less diverse and were predominantly dominant in <i>Allobaculum</i> .
Theis, et al. (21)	2020	Intestine, lung, oral cavity, vagina	Homogenized tissue or Eswab fluid was plated onto tryptic soy agar with 5% sheep blood and Chocolate agar plates under anoxic, hypoxic (5% CO <sub>2</sub> , 5% O <sub>2</sub> and 90% N <sub>2</sub> ), and oxic conditions at 37° C for 7 days.	C57BL/6	Several bacterial taxa abundant in the intestine included S24-7, <i>Candidatus Arthromitus, Bacteroides, Helicobacter, and Lactobacillus</i> . The lung was predominantly S24-7 and <i>Lactobacillus</i> . The oral cavity was abundant in <i>Streptococcus, Lactobacillus, and Pasteurellaceae</i> , while the vagina was almost exclusively <i>Pasteurellaceae</i> and <i>Helicobacter</i> .
Liu, et al. (121)	2021	Intestine	Not performed	ICR	Abundant taxa in the control group included <i>Prevotellaceae</i> and <i>Acinetobacter</i> and were primarily composed of members of Firmicutes and Bacteroidetes phyla

846

847 **Table 2. Global comparisons of the cultured murine microbiota.**

Beta diversity	Composition			Structure			848
	F	R <sup>2</sup>	p	F	R <sup>2</sup>	p	849
<b>Mouse ID</b>	1.123	0.081	0.059	1.214	0.078	0.125	
<b>Body site</b>	6.389	0.138	<b>0.001</b>	7.497	0.145	<b>0.001</b>	850
<b>Atmosphere</b>	2.541	0.037	<b>0.001</b>	5.576	0.072	<b>0.001</b>	851
<b>ID * Body site</b>	0.986	0.199	0.556	1.231	0.222	0.058	
<b>ID * Atmosphere</b>	1.081	0.156	0.073	1.091	0.140	<b>0.002</b>	852
<b>Body site * Atmosphere</b>	1.538	0.066	<b>0.001</b>	1.396	0.054	0.056	

853

854 **Table 3. Global (A) and pairwise (B) comparisons of the cultured murine microbiota after**  
 855 **bioinformatically pooling data across atmospheres by body site for each individual mouse.**

856

A	Global	Composition			Structure			853
		F	R <sup>2</sup>	p	F	R <sup>2</sup>	p	
	Mouse ID	1.348	0.314	<b>0.002</b>	2.056	0.395	<b>0.001</b>	
	Body site	3.171	0.221	<b>0.001</b>	3.833	0.221	<b>0.001</b>	
	Body site controlled for ID	3.044	0.233	<b>0.001</b>	3.290	0.248	<b>0.001</b>	
B		Composition			Composition			
	Pairwise controlled for mouse ID	Oral cavity n = 9		Lung n = 7	Intestine n = 9		Vagina n = 9	
		F	R <sup>2</sup>	p	F	R <sup>2</sup>	p	F
	Oral cavity			1.90 0.12 <b>0.016</b>	5.29 0.25 <b>0.004</b>		2.45 0.13 <b>0.004</b>	
Structure	Lung	2.16	0.13	<b>0.016</b>				3.40 0.20 <b>0.016</b> 1.27 0.08 0.094
	Intestine	5.28	0.25	<b>0.004</b>	3.60 0.20 <b>0.016</b>			4.10 0.20 <b>0.004</b>
	Vagina	2.48	0.13	0.059	1.97 0.12 0.094	4.43 0.22 <b>0.008</b>		

857

858 **Table 4. Correlations between cultured microbiota recovered under anoxic, hypoxic, oxic**  
 859 **atmospheres, or after pooling data from all three atmospheres, and molecular 16S rRNA**  
 860 **gene profiles.**

	Anoxic		Hypoxic		Oxic		Pooled Atmospheres	
	r	p	r	p	r	p	r	p
Oral cavity	-0.1185	0.7717	-0.5196	0.8655	-0.123	0.7409	-0.0662	0.6316
Intestine	0.4847	0.0616	<b>0.3982</b>	<b>0.0486</b>	<b>0.6139</b>	<b>0.0123</b>	<b>0.5511</b>	<b>0.0212</b>
Vagina	<b>0.4564</b>	<b>0.0072</b>	<b>0.747</b>	<b>0.0003</b>	<b>0.7149</b>	<b>0.0003</b>	<b>0.6965</b>	<b>0.0007</b>

861 Spearman rank correlation coefficients (r) and corresponding p values are provided. The lung could not be assessed due to low sample size.

862

863 **FIGURE LEGENDS**

864 **Figure 1. Study design for characterizing the microbiota of the oral cavity, intestine, lung,**

865 **and vagina of pregnant mice.** Briefly, two sets of samples were collected from each body site

866 of 11 pregnant mice. One set of samples was used for culture and the other for molecular

867 surveys. Cultures were performed on samples from each body site, under three different

868 atmospheric conditions on multiple media types. Bacterial growth from each plate type was

869 collected by plate washing with sterile PBS and then combined under each atmosphere. These

870 samples subsequently had their DNA extracted followed by 16S rRNA gene amplification and

871 sequencing. After classification of 16S rRNA gene sequences through DADA2, culture profiles

872 for each body site under each atmosphere were generated as well as overall body site culture

873 profiles after pooling the sequence data from all three atmospheres. Samples for molecular

874 surveys had their DNA extracted directly from the samples followed by 16S rRNA gene

875 amplification, sequencing, and classification to generate molecular profiles.

876 **Figure 2. Alpha diversity comparisons between the microbiota cultured under different**

877 **atmospheres for the oral cavity, lung, intestine, and vagina and between body sites.** Bar

878 plots indicate differences in three alpha diversity measures among anoxic, hypoxic, and oxic

879 cultures of the oral cavity (A), lung (B), intestine (C), and vagina (D), as well as across body

880 sites (E). For panel E, culture data from each atmosphere for each individual mouse by body site

881 were bioinformatically pooled, and only mice with culture data from all body sites and all

882 atmospheres ( $N = 5$ ) were included in the analyses. Data points are color-coded by mouse ID and

883 are consistent across panels. Lower case letters that are shared within each panel indicate

884 pairwise comparisons that were not significant.

885 **Figure 3. Comparisons of cultured microbiota from the oral cavity, lung, intestine, and**

886 **vagina, controlled for atmosphere.** Panels A and B contain Principal Coordinates Analysis

887 (PCoA) plots illustrating variation among cultured microbiota of the oral cavity, lung, intestine

888 and vagina using Jaccard dissimilarity index (A) for composition and Bray-Curtis dissimilarity

889 index (B) for structure. Ellipses in (A) and (B) indicate standard deviation. The heatmap in panel

890 C includes ASVs  $\geq 1\%$  average relative abundance within a single body site and samples are

891 clustered by Bray-Curtis similarities within each body site. In panel D, LEfSe analysis identified

892 taxa preferentially recovered in a particular body site.

893 **Figure 4. Comparisons of sequenced microbiota and cultured microbiota from the oral**

894 **cavity, lung, intestine, and vagina.** The heatmap in panel A represents log transformed precent

895 relative abundances. In panel B, molecular and culture profiles were separately averaged with

896 dots indicating whether an ASV was detected in culture. ASVs were included if they were  $\geq 1\%$

897 average relative abundance in the molecular profiles in one of the four body sites.

898 **Figure 5. Phylogenomic and KEGG analysis of two vaginal *Rodentibacter* isolates.** In panel

899 A, the phylogenomic tree includes the *Rodentibacter* isolates ASV 2 and ASV 5 and all

900 *Rodentibacter* type strains and in panel B, all published *Rodentibacter* genomes are included.

901 Panels C and D summarize the distribution of functional KEGG pathways enriched in the

902 genomes of the two isolates. Phylogenomic trees were constructed by comparing 92 conserved  
903 bacterial genes as described by Na et al. (112).

904

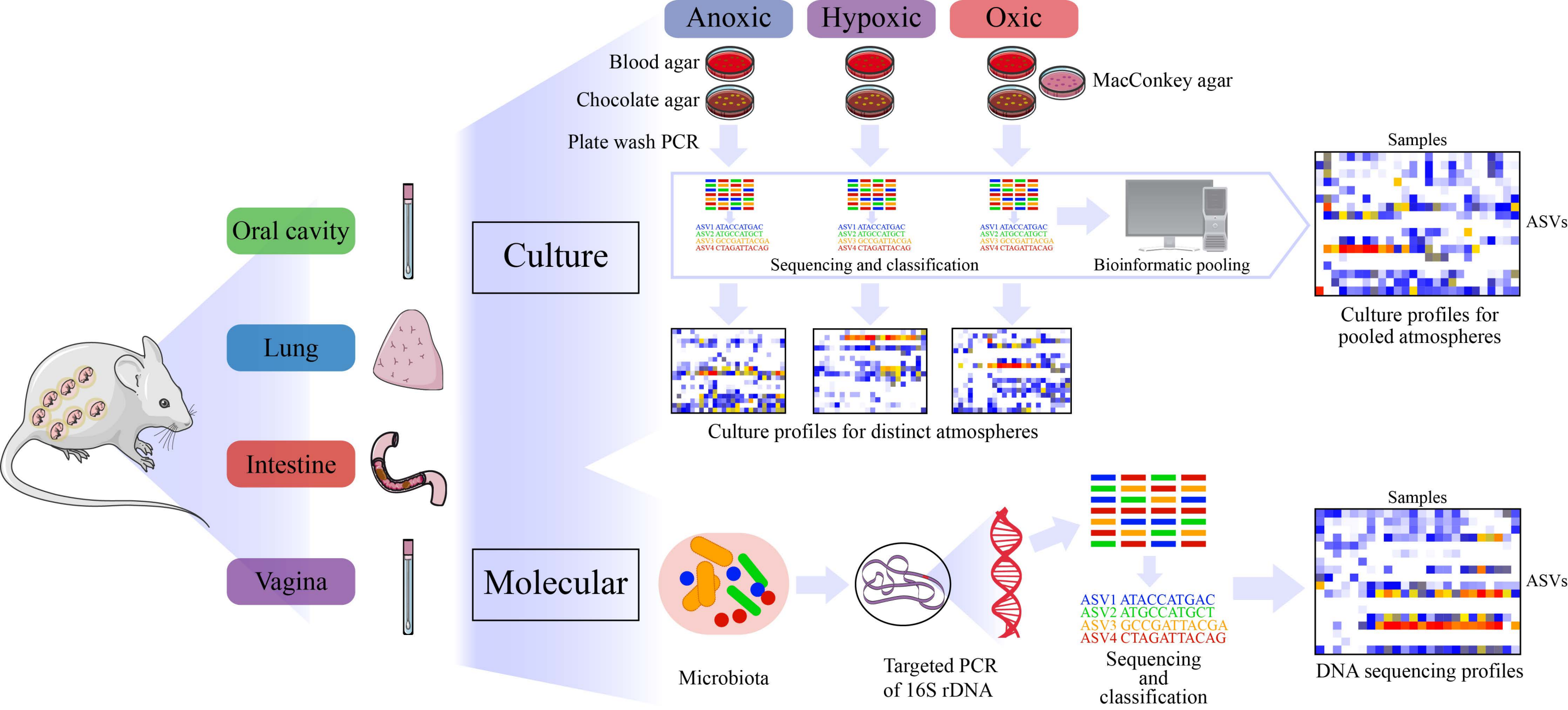
905

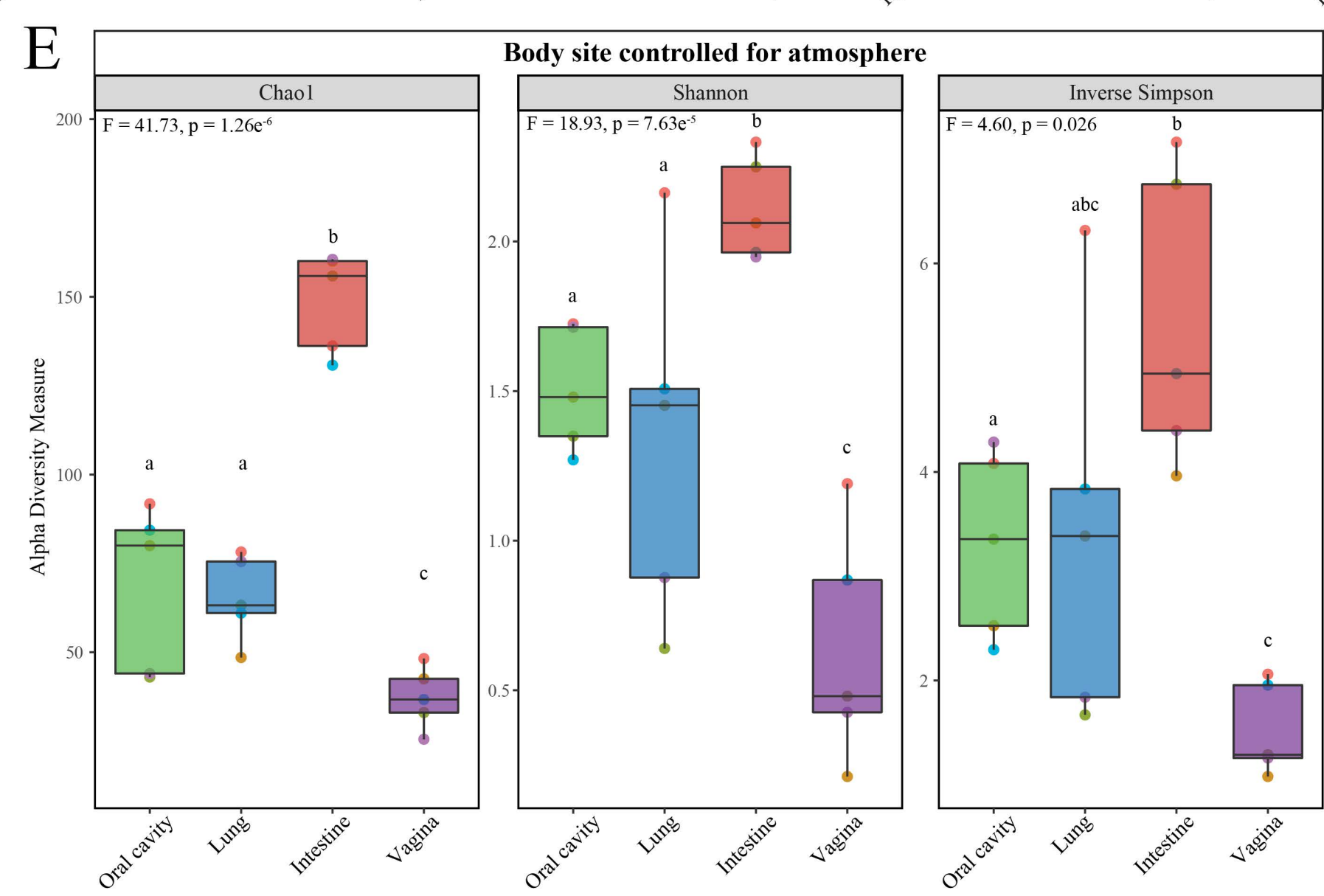
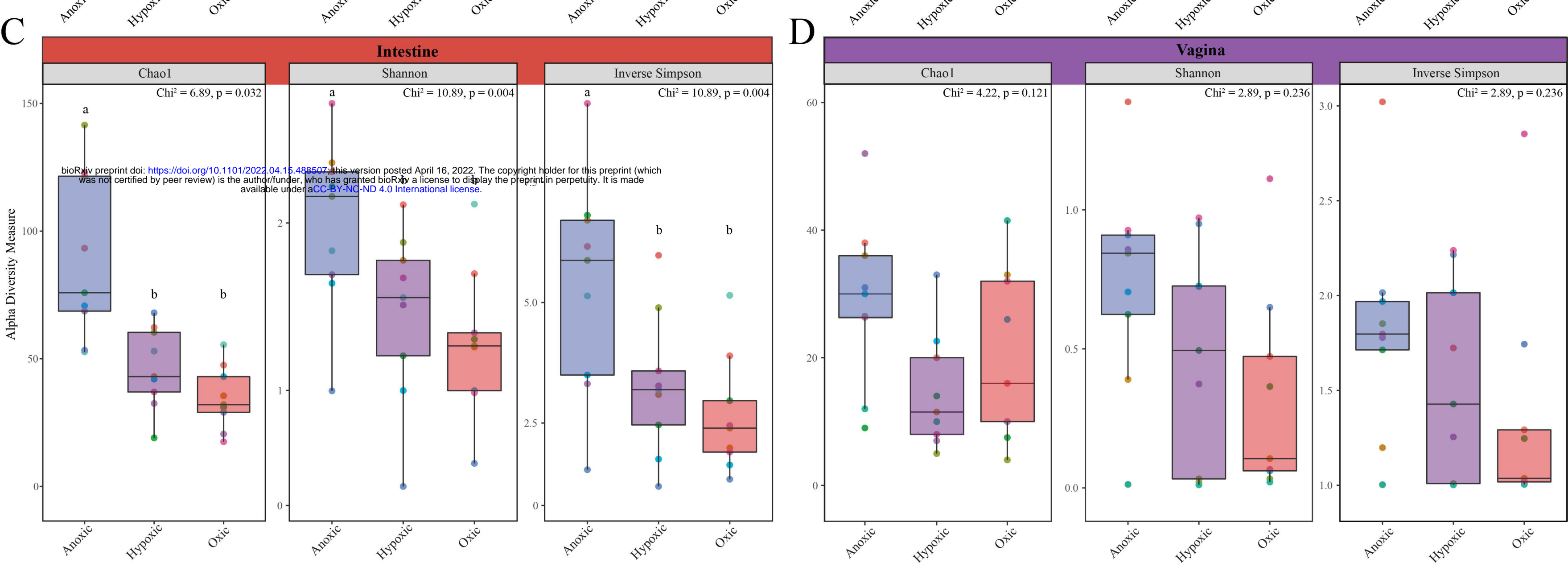
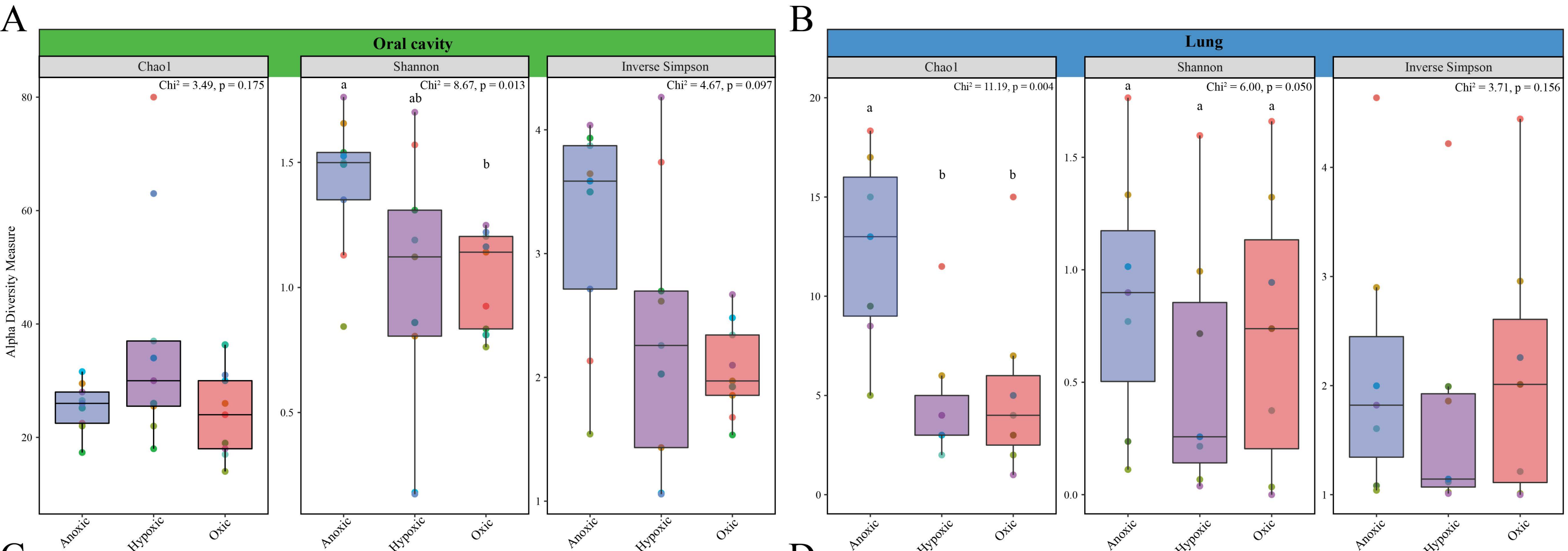
906

907

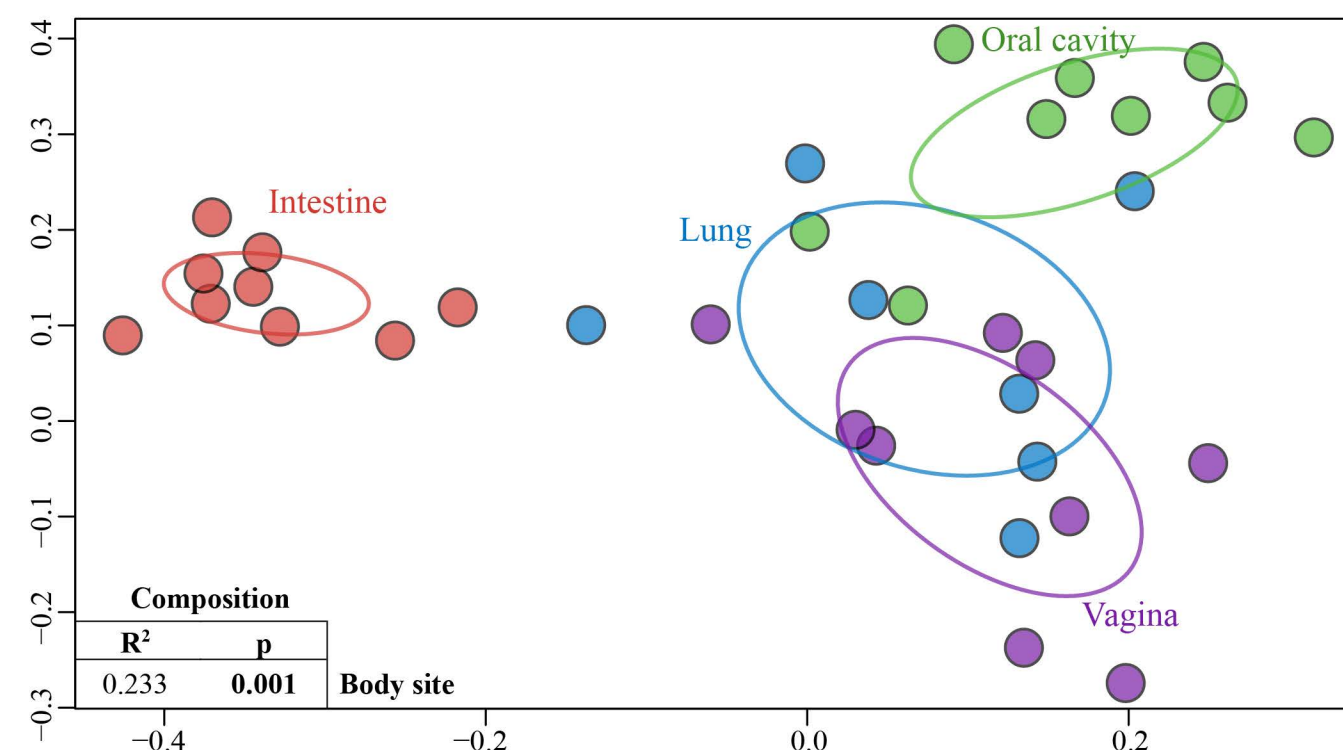
908

909

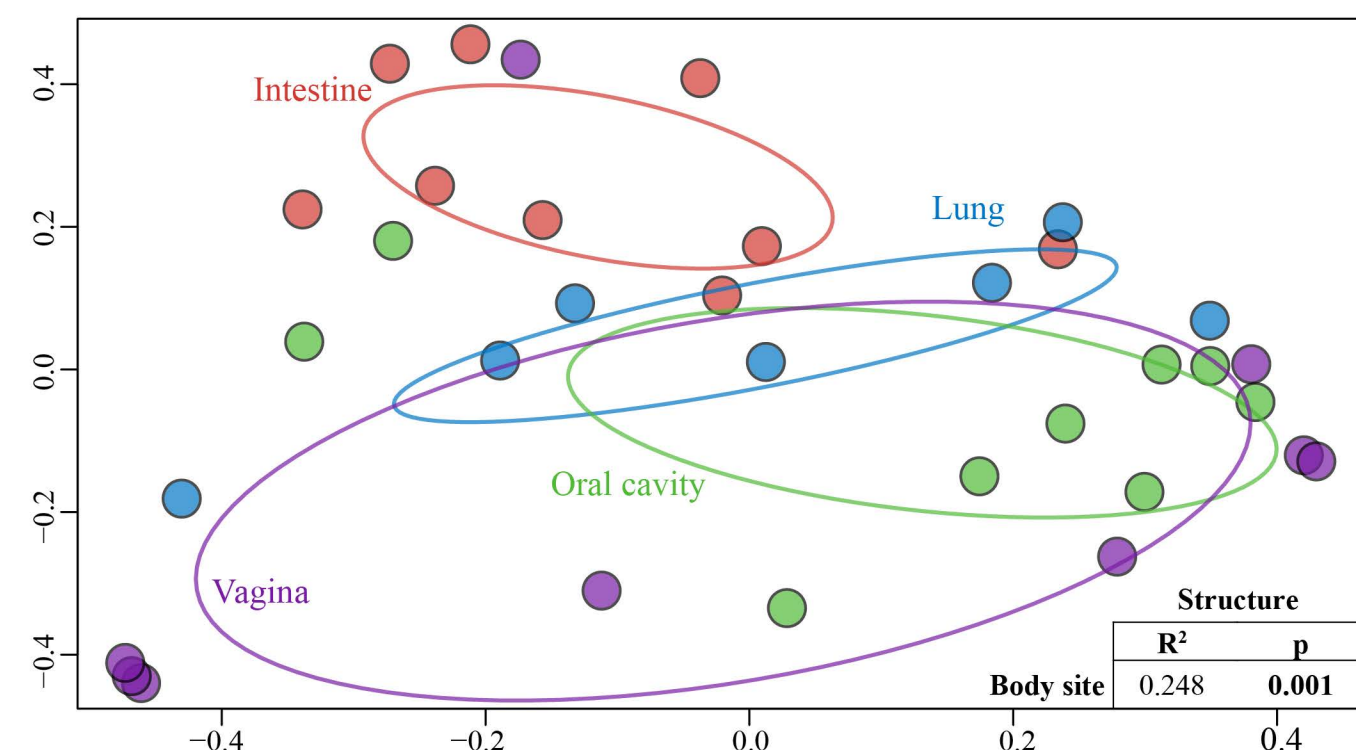




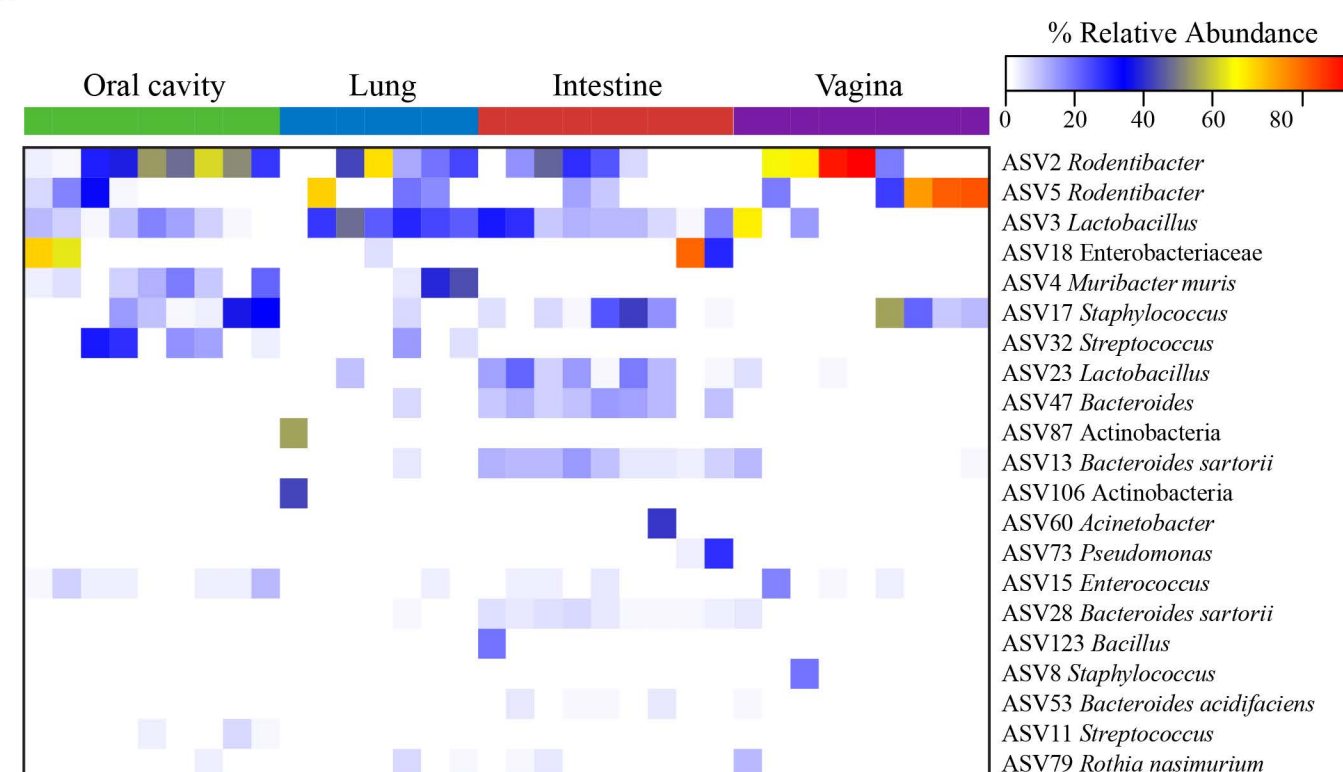
A



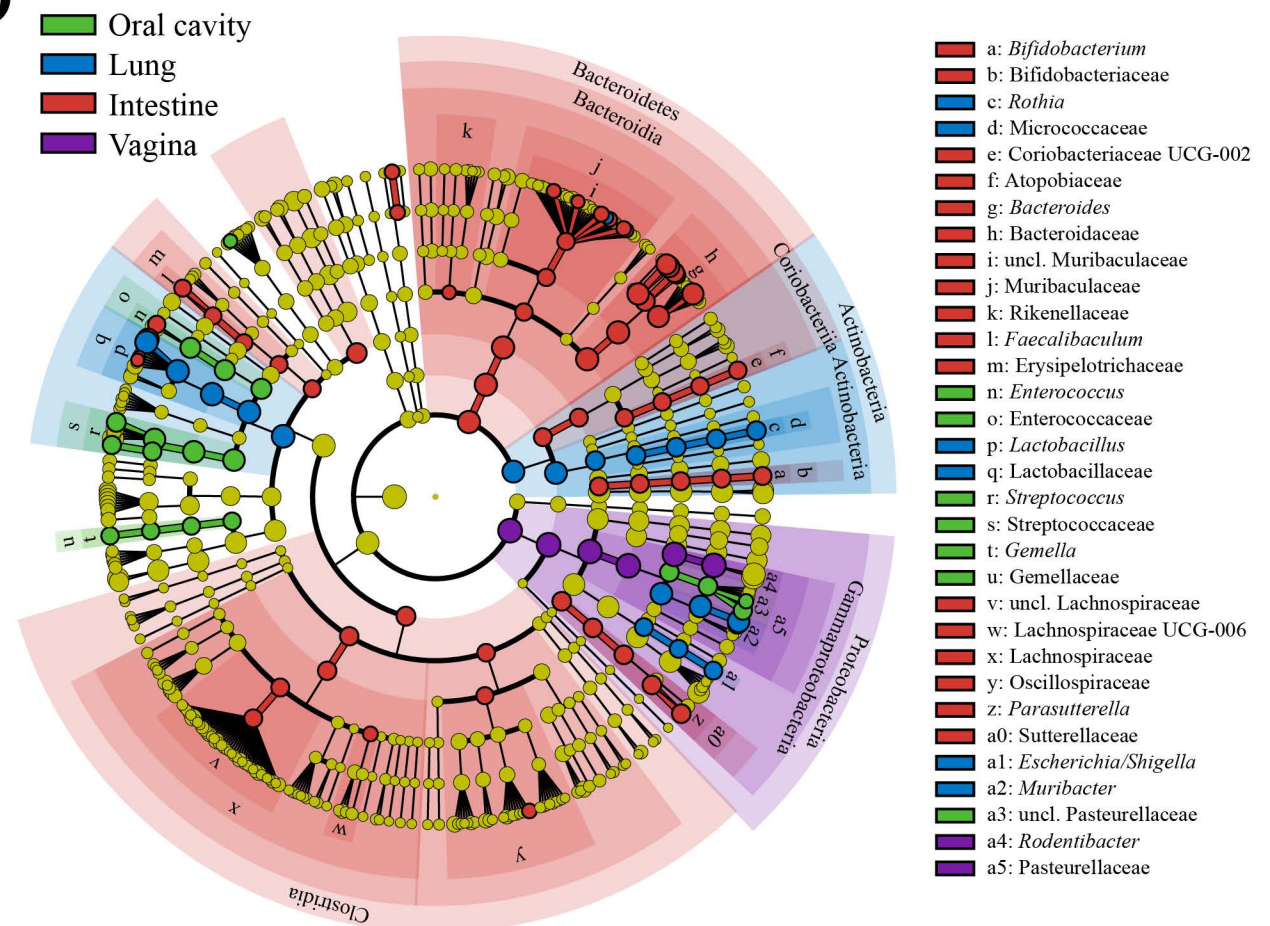
B



C



D



**A**

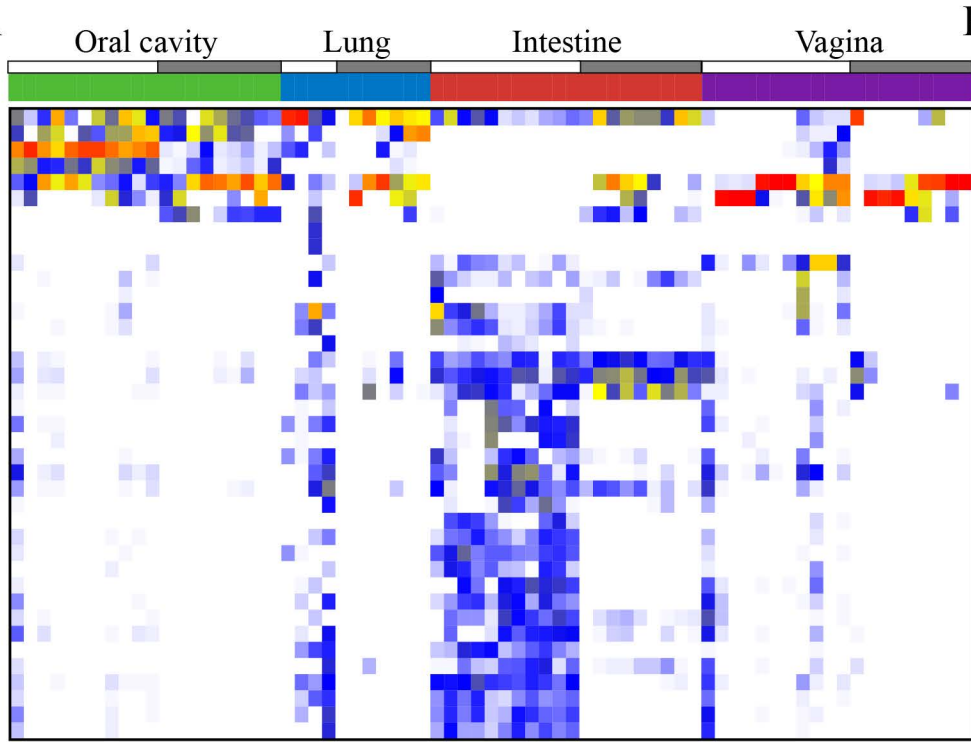
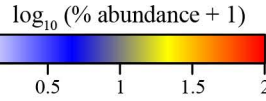
Oral cavity

Lung

Intestine

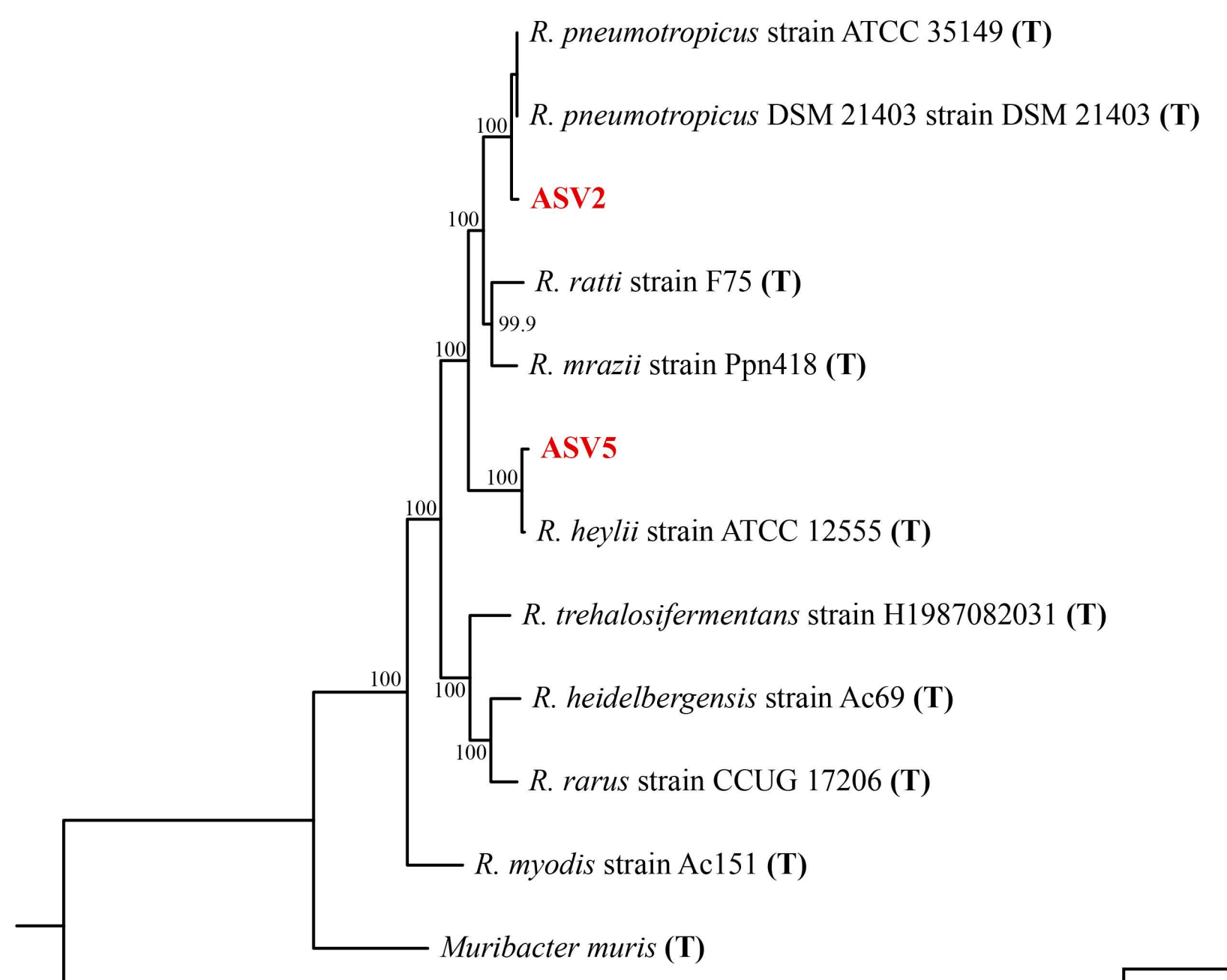
Vagina

- Molecular profile
- Culture profile
- Recovered in culture

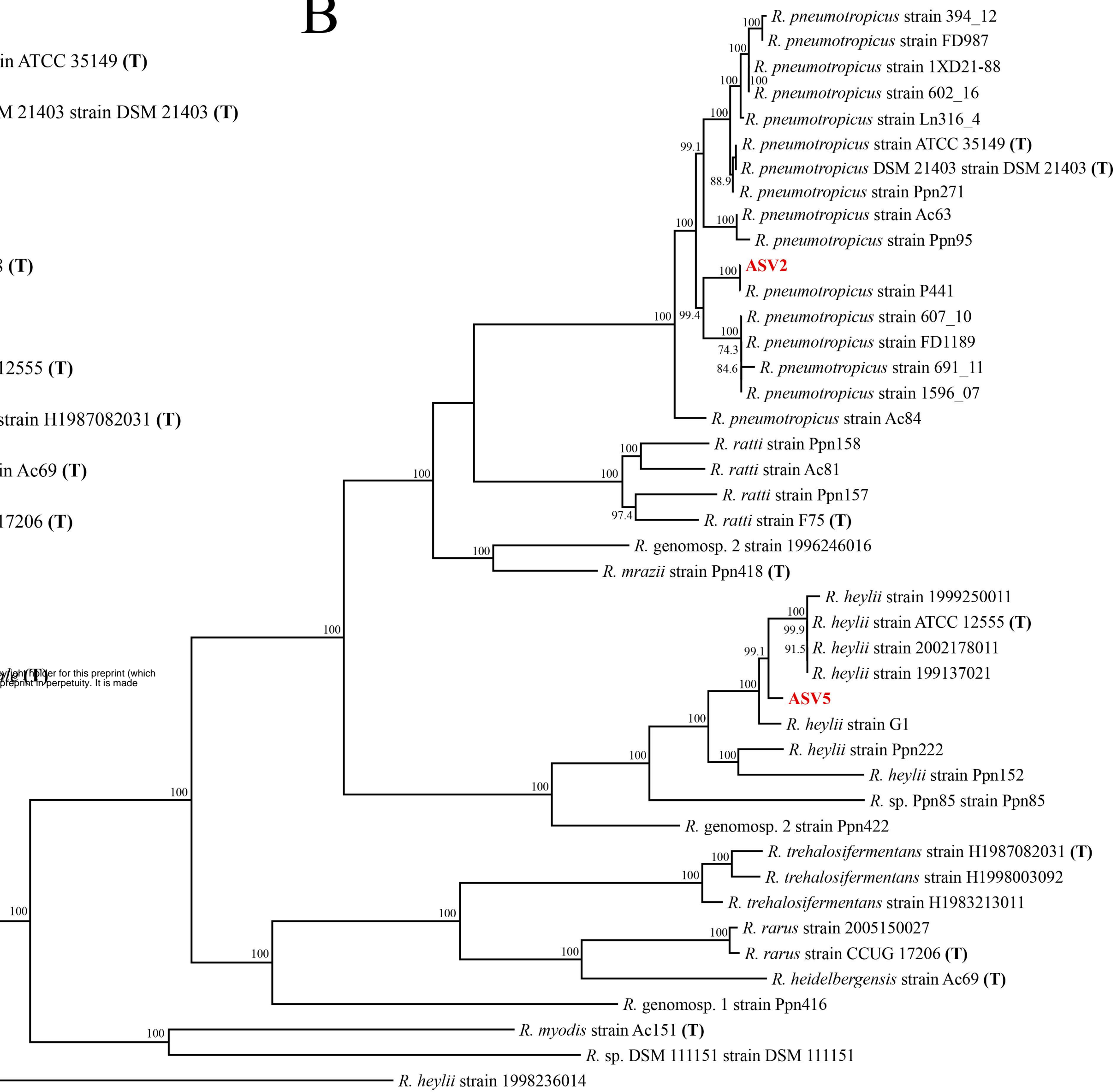
**B**

- ASV3 *Lactobacillus*
- ASV4 *Muribacter muris*
- ASV1 *Streptococcus danieliae*
- ASV11 *Streptococcus*
- ASV2 *Rodentibacter*
- ASV5 *Rodentibacter*
- ASV15 *Enterococcus*
- ASV21 *Listeria*
- ASV1047 *Cardiobacterium hominis*
- ASV49 *Helicobacter hepaticus*
- ASV41 *Bifidobacterium*
- ASV68 *Lachnospiraceae*
- ASV12 *Muribaculaceae*
- ASV25 *Muribaculaceae*
- ASV133 *Lachnospiraceae*
- ASV28 *Bacteroides sartorii*
- ASV13 *Bacteroides sartorii*
- ASV23 *Lactobacillus*
- ASV42 *Lachnospiraceae*
- ASV22 *Lachnospiraceae*
- ASV36 *Lachnospiraceae NK4A136 group*
- ASV37 *Desulfovibrionaceae*
- ASV16 *Helicobacter ganmani*
- ASV20 *Parasutterella*
- ASV43 *Akkermansia muciniphila*
- ASV52 *Alistipes*
- ASV39 *Muribaculaceae*
- ASV30 *Candidatus Arthromitus*
- ASV46 *Lachnospiraceae UCG-006*
- ASV24 *Lachnospiraceae NK4A136 group*
- ASV31 *Muribaculaceae*
- ASV26 *Bacteroides acidifaciens*
- ASV27 *Prevotellaceae*
- ASV40 *Desulfovibrio*
- ASV35 *Faecalibaculum*
- ASV19 *Muribaculaceae*
- ASV33 *Muribaculaceae*
- ASV29 *Muribaculaceae*
- ASV34 *Muribaculaceae*

A

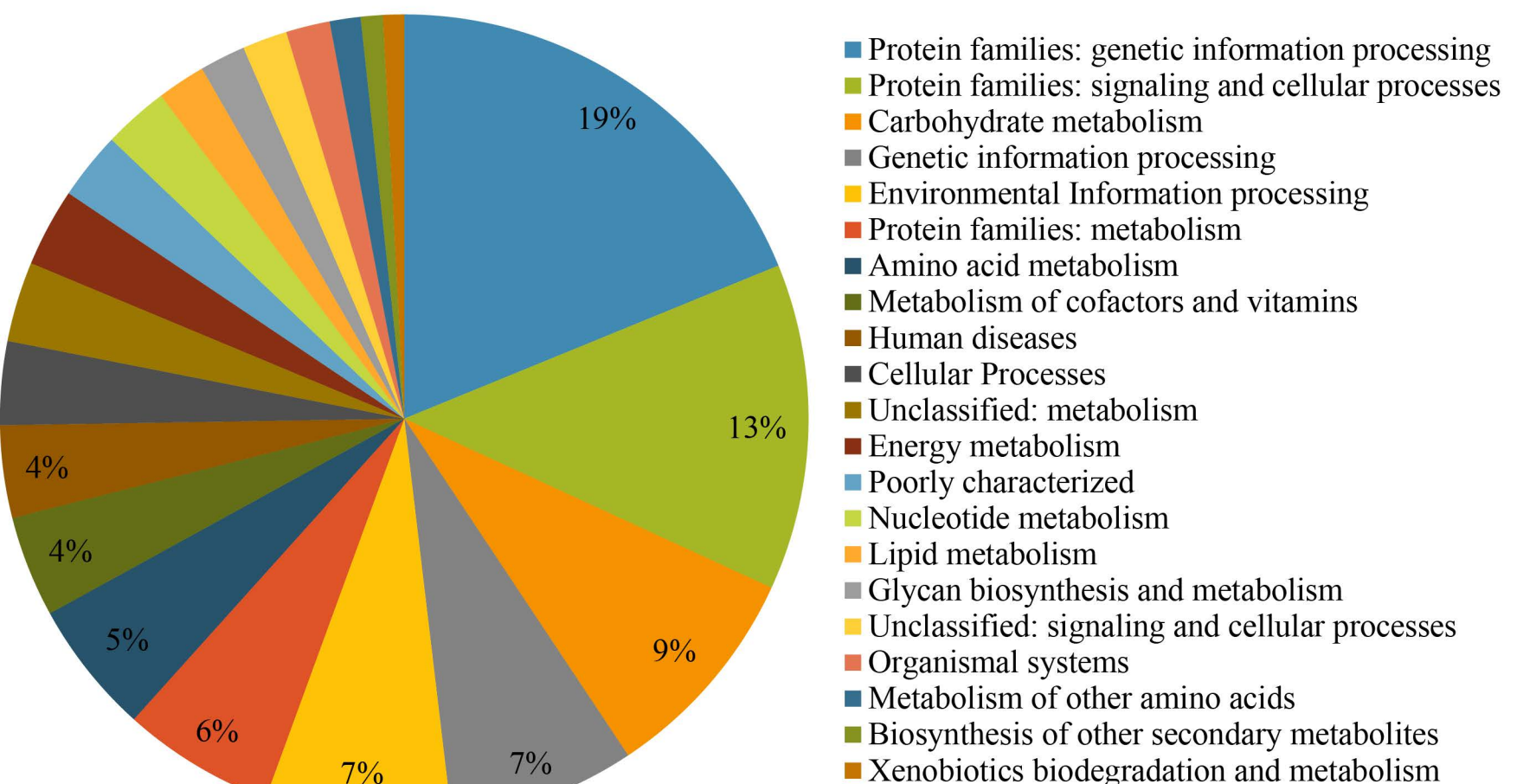


B



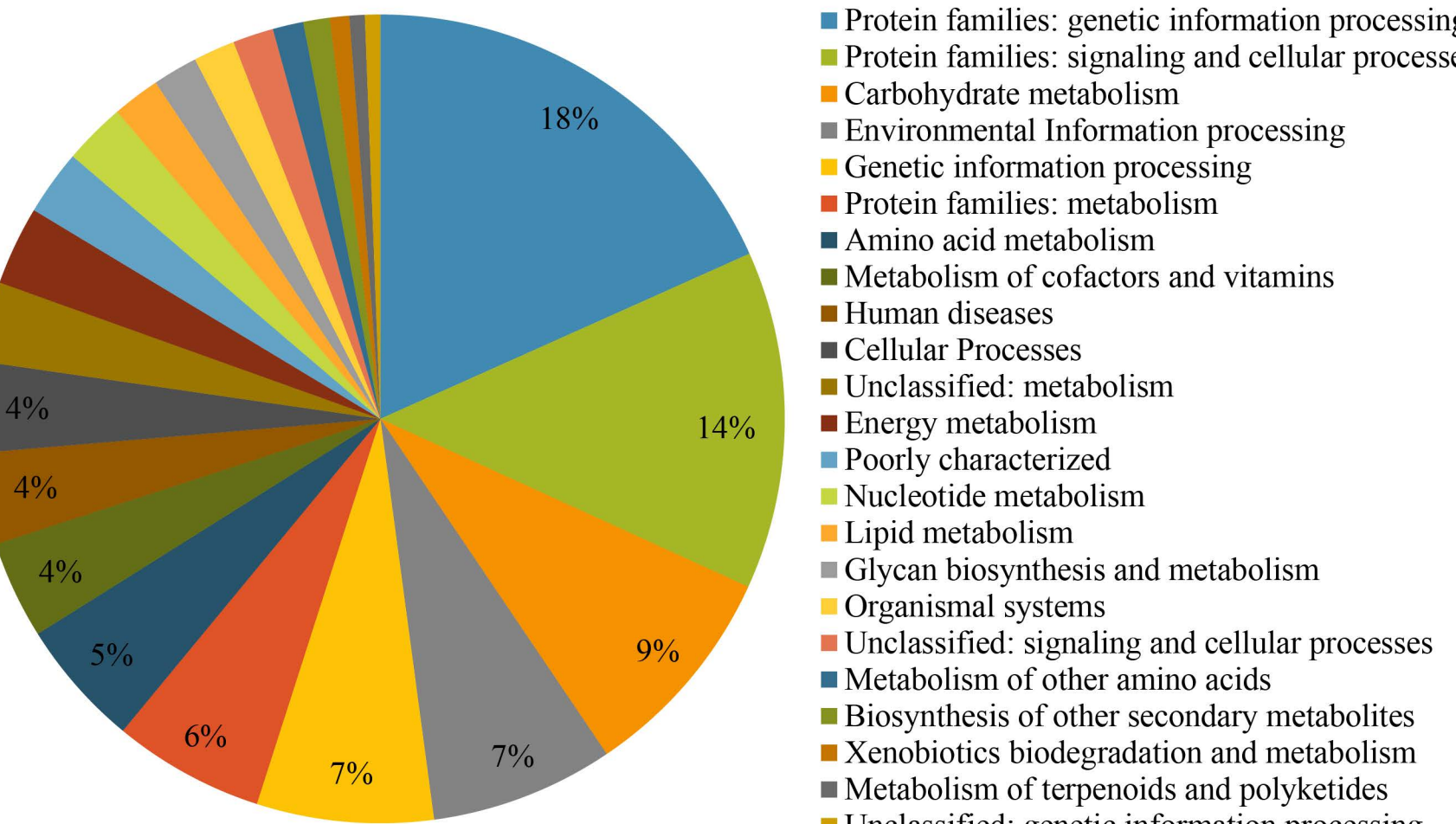
C

### *Rodentibacter pneumotropicus* ASV2 genome



D

### *Rodentibacter heylii* ASV5 genome



910 **REFERENCES**

- 911 1. Krych L, Hansen CHF, Hansen AK, van den Berg FWJ, Nielsen DS. 2013.  
912 Quantitatively different, yet qualitatively alike: a meta-analysis of the mouse core gut  
913 microbiome with a view towards the human gut microbiome. *PLOS ONE* 8:e62578-  
914 e62578.
- 915 2. Walter J, Armet AM, Finlay BB, Shanahan F. 2020. Establishing or Exaggerating  
916 Causality for the Gut Microbiome: Lessons from Human Microbiota-Associated Rodents.  
917 *Cell* 180:221-232.
- 918 3. Nguyen TLA, Vieira-Silva S, Liston A, Raes J. 2015. How informative is the mouse for  
919 human gut microbiota research? *Disease models & mechanisms* 8:1-16.
- 920 4. Hugenholz F, de Vos WM. 2018. Mouse models for human intestinal microbiota  
921 research: a critical evaluation. *Cellular and molecular life sciences : CMLS* 75:149-160.
- 922 5. Barfod KK, Roggenbuck M, Hansen LH, Schjørring S, Larsen ST, Sørensen SJ, Krogfelt  
923 KA. 2013. The murine lung microbiome in relation to the intestinal and vaginal bacterial  
924 communities. *BMC microbiology* 13:303-303.
- 925 6. Dollive S, Chen YY, Grunberg S, Bittinger K, Hoffmann C, Vandivier L, Bushman FD.  
926 2013. Fungi of the murine gut: episodic variation and proliferation during antibiotic  
927 treatment. *PLOS ONE* 8.
- 928 7. Albenberg L, Esipova TV, Judge CP, Bittinger K, Chen J, Laughlin A, Grunberg S,  
929 Baldassano RN, Lewis JD, Li H, Thom SR, Bushman FD, Vinogradov SA, Wu GD.  
930 2014. Correlation Between Intraluminal Oxygen Gradient and Radial Partitioning of  
931 Intestinal Microbiota. *Gastroenterology* 147:1055-1063.e8.
- 932 8. Braniste V, Al-Asmakh M, Kowal C, Anuar F, Abbaspour A, Tóth M, Korecka A,  
933 Bakocic N, Ng LG, Kundu P, Gulyás B, Halldin C, Hultenby K, Nilsson H, Hebert H,  
934 Volpe BT, Diamond B, Pettersson S. 2014. The gut microbiota influences blood-brain  
935 barrier permeability in mice. *Sci Transl Med* 6:263ra158.
- 936 9. Koenigsknecht MJ, Theriot CM, Bergin IL, Schumacher CA, Schloss PD, Young VB.  
937 2015. Dynamics and Establishment of *Clostridium difficile* Infection in the Murine  
938 Gastrointestinal Tract. *Infection and Immunity* 83:934-941.
- 939 10. Laukens D, Brinkman BM, Raes J, Vos M, Vandenabeele P. 2016. Heterogeneity of the  
940 gut microbiome in mice: guidelines for optimizing experimental design. *FEMS Microbiol  
941 Rev* 40.
- 942 11. Lagkouvardos I, Pukall R, Abt B, Foesel BU, Meier-Kolthoff JP, Kumar N, Bresciani A,  
943 Martínez I, Just S, Ziegler C, Brugiroux S, Garzetti D, Wenning M, Bui TPN, Wang J,  
944 Hugenholz F, Plugge CM, Peterson DA, Hornef MW, Baines JF, Smidt H, Walter J,  
945 Kristiansen K, Nielsen HB, Haller D, Overmann J, Stecher B, Clavel T. 2016. The Mouse  
946 Intestinal Bacterial Collection (miBC) provides host-specific insight into cultured  
947 diversity and functional potential of the gut microbiota. *Nature Microbiology* 1:16131.
- 948 12. Tochitani S, Ikeno T, Ito T, Sakurai A, Yamauchi T, Matsuzaki H. 2016. Administration  
949 of Non-Absorbable Antibiotics to Pregnant Mice to Perturb the Maternal Gut Microbiota  
950 Is Associated with Alterations in Offspring Behavior. *PLOS ONE* 11:e0138293.
- 951 13. Elderman M, Hugenholz F, Belzer C, Boekschoten M, de Haan B, de Vos P, Faas M.  
952 2018. Changes in intestinal gene expression and microbiota composition during late  
953 pregnancy are mouse strain dependent. *Scientific Reports* 8:10001.

954 14. Wang J, Lang T, Shen J, Dai J, Tian L, Wang X. 2019. Core Gut Bacteria Analysis of  
955 Healthy Mice. *Frontiers in Microbiology* 10.

956 15. Vuong HE, Pronovost GN, Williams DW, Coley EJL, Siegler EL, Qiu A, Kazantsev M,  
957 Wilson CJ, Rendon T, Hsiao EY. 2020. The maternal microbiome modulates fetal  
958 neurodevelopment in mice. *Nature* 586:281-286.

959 16. Ahern PP, Maloy KJ. 2020. Understanding immune-microbiota interactions in the  
960 intestine. *Immunology* 159:4-14.

961 17. Kimura I, Miyamoto J, Ohue-Kitano R, Watanabe K, Yamada T, Onuki M, Aoki R, Isobe  
962 Y, Kashihara D, Inoue D, Inaba A, Takamura Y, Taira S, Kumaki S, Watanabe M, Ito M,  
963 Nakagawa F, Irie J, Kakuta H, Shinohara M, Iwatsuki K, Tsujimoto G, Ohno H, Arita M,  
964 Itoh H, Hase K. 2020. Maternal gut microbiota in pregnancy influences offspring  
965 metabolic phenotype in mice. *Science* 367:eaaw8429.

966 18. Karpinets TV, Solley TN, Mikkelsen MD, Dorta-Estremera S, Nookala SS, Medrano  
967 AYD, Petrosino JF, Mezzari MP, Zhang J, Futreal PA, Sastry KJ, Colbert LE, Klopp A.  
968 2020. Effect of Antibiotics on Gut and Vaginal Microbiomes Associated with Cervical  
969 Cancer Development in Mice. *Cancer Prevention Research* 13:997-1006.

970 19. Mandal RK, Denny JE, Waide ML, Li Q, Bhutiani N, Anderson CD, Baby BV, Jala VR,  
971 Egilmez NK, Schmidt NW. 2020. Temporospatial shifts within commercial laboratory  
972 mouse gut microbiota impact experimental reproducibility. *BMC Biology* 18:83.

973 20. Chung YW, Gwak H-J, Moon S, Rho M, Ryu J-H. 2020. Functional dynamics of  
974 bacterial species in the mouse gut microbiome revealed by metagenomic and  
975 metatranscriptomic analyses. *PLOS ONE* 15:e0227886.

976 21. Theis KR, Romero R, Greenberg JM, Winters AD, Garcia-Flores V, Motomura K,  
977 Ahmad MM, Galaz J, Arenas-Hernandez M, Gomez-Lopez N. 2020. No Consistent  
978 Evidence for Microbiota in Murine Placental and Fetal Tissues. *mSphere* 5:e00933-19.

979 22. Dudley DJ, Branch DW, Edwin SS, Mitchell MD. 1996. Induction of preterm birth in  
980 mice by RU486. *Biol Reprod* 55:992-5.

981 23. Hirsch E, Blanchard R, Mehta SP. 1999. Differential fetal and maternal contributions to  
982 the cytokine milieu in a murine model of infection-induced preterm birth. *Am J Obstet  
983 Gynecol* 180:429-34.

984 24. Elovitz MA, Mrinalini C. 2006. The use of progestational agents for preterm birth:  
985 lessons from a mouse model. *Am J Obstet Gynecol* 195:1004-10.

986 25. Shynlova O, Nedd-Roderique T, Li Y, Dorogin A, Lye SJ. 2013. Myometrial immune  
987 cells contribute to term parturition, preterm labour and post-partum involution in mice. *J  
988 Cell Mol Med* 17:90-102.

989 26. Akgul Y, Word RA, Ensign LM, Yamaguchi Y, Lydon J, Hanes J, Mahendroo M. 2014.  
990 Hyaluronan in cervical epithelia protects against infection-mediated preterm birth. *J Clin  
991 Invest* 124:5481-9.

992 27. Rinaldi SF, Makieva S, Frew L, Wade J, Thomson AJ, Moran CM, Norman JE, Stock SJ.  
993 2015. Ultrasound-guided intrauterine injection of lipopolysaccharide as a novel model of  
994 preterm birth in the mouse. *Am J Pathol* 185:1201-6.

995 28. Vornhagen J, Quach P, Boldenow E, Merillat S, Whidbey C, Ngo LY, Adams Waldorf  
996 KM, Rajagopal L. 2016. Bacterial Hyaluronidase Promotes Ascending GBS Infection  
997 and Preterm Birth. *mBio* 7.

998 29. Gilman-Sachs A, Dambaeva S, Salazar Garcia MD, Hussein Y, Kwak-Kim J, Beaman K.  
999 2018. Inflammation induced preterm labor and birth. *J Reprod Immunol* 129:53-58.

1000 30. McCarthy R, Martin-Fairey C, Sojka DK, Herzog ED, Jungheim ES, Stout MJ, Fay JC,  
1001 Mahendroo M, Reese J, Herington JL, Plosa EJ, Shelton EL, England SK. 2018. Mouse  
1002 models of preterm birth: suggested assessment and reporting guidelines. *Biol Reprod*  
1003 99:922-937.

1004 31. Gomez-Lopez N, Romero R, Arenas-Hernandez M, Panaitescu B, Garcia-Flores V, Mial  
1005 TN, Sahi A, Hassan SS. 2018. Intra-amniotic administration of lipopolysaccharide  
1006 induces spontaneous preterm labor and birth in the absence of a body temperature  
1007 change. *J Matern Fetal Neonatal Med* 31:439-446.

1008 32. Lee JY, Song H, Dash O, Park M, Shin NE, McLane MW, Lei J, Hwang JY, Burd I.  
1009 2019. Administration of melatonin for prevention of preterm birth and fetal brain injury  
1010 associated with premature birth in a mouse model. *Am J Reprod Immunol* 82:e13151.

1011 33. Nold C, Stone J, O'Hara K, Davis P, Kiveliyk V, Blanchard V, Yellon SM, Vella AT.  
1012 2019. Block of Granulocyte-Macrophage Colony-Stimulating Factor Prevents  
1013 Inflammation-Induced Preterm Birth in a Mouse Model for Parturition. *Reprod Sci*  
1014 26:551-559.

1015 34. Motomura K, Romero R, Xu Y, Theis KR, Galaz J, Winters AD, Slutsky R, Garcia-  
1016 Flores V, Zou C, Levenson D, Para R, Ahmad MM, Miller D, Hsu CD, Gomez-Lopez N.  
1017 2020. Intra-Amniotic Infection with *Ureaplasma parvum* Causes Preterm Birth and  
1018 Neonatal Mortality That Are Prevented by Treatment with Clarithromycin. *mBio* 11.

1019 35. Gomez-Lopez N, Arenas-Hernandez M, Romero R, Miller D, Garcia-Flores V, Leng Y,  
1020 Xu Y, Galaz J, Hassan SS, Hsu CD, Tse H, Sanchez-Torres C, Done B, Tarca AL. 2020.  
1021 Regulatory T Cells Play a Role in a Subset of Idiopathic Preterm Labor/Birth and  
1022 Adverse Neonatal Outcomes. *Cell Rep* 32:107874.

1023 36. Fan C, Dai Y, Zhang L, Rui C, Wang X, Luan T, Fan Y, Dong Z, Hou W, Li P, Liao Q,  
1024 Zeng X. 2021. Aerobic Vaginitis Induced by *Escherichia coli* Infection During Pregnancy  
1025 Can Result in Adverse Pregnancy Outcomes Through the IL-4/JAK-1/STAT-6 Pathway.  
1026 *Front Microbiol* 12:651426.

1027 37. Spencer NR, Radnaa E, Baljinnyam T, Kechichian T, Tantengco OAG, Bonney E,  
1028 Kammala AK, Sheller-Miller S, Menon R. 2021. Development of a mouse model of  
1029 ascending infection and preterm birth. *PLOS ONE* 16:e0260370.

1030 38. Gershater M, Romero R, Arenas-Hernandez M, Galaz J, Motomura K, Tao L, Xu Y,  
1031 Miller D, Pique-Regi R, Martinez G, 3rd, Liu Y, Jung E, Para R, Gomez-Lopez N. 2022.  
1032 IL-22 Plays a Dual Role in the Amniotic Cavity: Tissue Injury and Host Defense against  
1033 Microbes in Preterm Labor. *J Immunol* 208:1595-1615.

1034 39. Faas MM, Liu Y, Borghuis T, van Loo-Bouwman CA, Harmsen H, de Vos P. 2019.  
1035 Microbiota Induced Changes in the Immune Response in Pregnant Mice. *Front Immunol*  
1036 10:2976.

1037 40. Gravett MG, Hummel D, Eschenbach DA, Holmes KK. 1986. Preterm labor associated  
1038 with subclinical amniotic fluid infection and with bacterial vaginosis. *Obstet Gynecol*  
1039 67:229-37.

1040 41. Krohn MA, Hillier SL, Nugent RP, Cotch MF, Carey JC, Gibbs RS, Eschenbach DA.  
1041 1995. The genital flora of women with intraamniotic infection. *Vaginal Infection and*  
1042 *Prematurity Study Group. J Infect Dis* 171:1475-80.

1043 42. Romero R, Gomez-Lopez N, Winters AD, Jung E, Shaman M, Bieda J, Panaitescu B,  
1044 Pacora P, Erez O, Greenberg JM, Ahmad MM, Hsu CD, Theis KR. 2019. Evidence that

1045 intra-amniotic infections are often the result of an ascending invasion - a molecular  
1046 microbiological study. *J Perinat Med* 47:915-931.

1047 43. Cobo T, Vergara A, Collado MC, Casals-Pascual C, Herreros E, Bosch J, Sánchez-García  
1048 AB, López-Parellada R, Ponce J, Gratacós E. 2019. Characterization of vaginal  
1049 microbiota in women with preterm labor with intra-amniotic inflammation. *Sci Rep*  
1050 9:18963.

1051 44. Eschenbach DA, Gravett MG, Chen KC, Hoyme UB, Holmes KK. 1984. Bacterial  
1052 vaginosis during pregnancy. An association with prematurity and postpartum  
1053 complications. *Scand J Urol Nephrol Suppl* 86:213-22.

1054 45. Holst E, Goffeng AR, Andersch B. 1994. Bacterial vaginosis and vaginal microorganisms  
1055 in idiopathic premature labor and association with pregnancy outcome. *J Clin Microbiol*  
1056 32:176-86.

1057 46. Hillier SL, Nugent RP, Eschenbach DA, Krohn MA, Gibbs RS, Martin DH, Cotch MF,  
1058 Edelman R, Pastorek JG, 2nd, Rao AV, et al. 1995. Association between bacterial  
1059 vaginosis and preterm delivery of a low-birth-weight infant. The Vaginal Infections and  
1060 Prematurity Study Group. *N Engl J Med* 333:1737-42.

1061 47. Meis PJ, Goldenberg RL, Mercer B, Moawad A, Das A, McNellis D, Johnson F, Iams  
1062 JD, Thom E, Andrews WW. 1995. The preterm prediction study: significance of vaginal  
1063 infections. National Institute of Child Health and Human Development Maternal-Fetal  
1064 Medicine Units Network. *Am J Obstet Gynecol* 173:1231-5.

1065 48. Nelson DB, Bellamy S, Nachamkin I, Ness RB, Macones GA, Allen-Taylor L. 2007.  
1066 First trimester bacterial vaginosis, individual microorganism levels, and risk of second  
1067 trimester pregnancy loss among urban women. *Fertility and Sterility* 88:1396-1403.

1068 49. Giraldo PC, Araujo ED, Junior JE, do Amaral RL, Passos MR, Goncalves AK. 2012. The  
1069 prevalence of urogenital infections in pregnant women experiencing preterm and full-  
1070 term labor. *Infect Dis Obstet Gynecol* 2012:878241.

1071 50. Romero R, Hassan SS, Gajer P, Tarca AL, Fadrosh DW, Bieda J, Chaemsathong P,  
1072 Miranda J, Chaiworapongsa T, Ravel J. 2014. The vaginal microbiota of pregnant women  
1073 who subsequently have spontaneous preterm labor and delivery and those with a normal  
1074 delivery at term. *Microbiome* 2:18.

1075 51. Digiulio DB, Callahan BJ, McMurdie PJ, Costello EK, Lyell DJ, Robaczewska A, Sun  
1076 CL, Gotsman DSA, Wong RJ, Shaw G, Stevenson DK, Holmes SP, Relman DA. 2015.  
1077 Temporal and spatial variation of the human microbiota during pregnancy. *Proceedings  
1078 of the National Academy of Sciences* 112:11060-11065.

1079 52. Cox C, Saxena N, Watt AP, Gannon C, McKenna JP, Fairley DJ, Sweet D, Shields MD,  
1080 Cosby SL, Coyle PV. 2016. The common vaginal commensal bacterium *Ureaplasma*  
1081 *parvum* is associated with chorioamnionitis in extreme preterm labor. *Journal of  
1082 Maternal-Fetal & Neonatal Medicine* 29:3646-3651.

1083 53. Haque MM, Merchant M, Kumar PN, Dutta A, Mande SS. 2017. First-trimester vaginal  
1084 microbiome diversity: A potential indicator of preterm delivery risk. *Scientific Reports* 7.

1085 54. Elovitz MA, Gajer P, Riis V, Brown AG, Humphrys MS, Holm JB, Ravel J. 2019.  
1086 Cervicovaginal microbiota and local immune response modulate the risk of spontaneous  
1087 preterm delivery. *Nat Commun* 10:1305.

1088 55. Fettweis JM, Serrano MG, Brooks JP, Edwards DJ, Girerd PH, Parikh HI, Huang B,  
1089 Arodz TJ, Edupuganti L, Glascock AL, Xu J, Jimenez NR, Vivadelli SC, Fong SS, Sheth  
1090 NU, Jean S, Lee V, Bokhari YA, Lara AM, Mistry SD, Duckworth RA, 3rd, Bradley SP,

1091 Koparde VN, Orenda XV, Milton SH, Rozycki SK, Matveyev AV, Wright ML,  
1092 Huzurbazar SV, Jackson EM, Smirnova E, Korlach J, Tsai YC, Dickinson MR, Brooks  
1093 JL, Drake JI, Chaffin DO, Sexton AL, Gravett MG, Rubens CE, Wijesooriya NR,  
1094 Hendricks-Muñoz KD, Jefferson KK, Strauss JF, 3rd, Buck GA. 2019. The vaginal  
1095 microbiome and preterm birth. *Nat Med* 25:1012-1021.

1096 56. Zhang F, Zhang T, Ma Y, Huang Z, He Y, Pan H, Fang M, Ding H. 2019. Alteration of  
1097 vaginal microbiota in patients with unexplained recurrent miscarriage. *Experimental and*  
1098 *therapeutic medicine* 17:3307-3316.

1099 57. Al-Memar M, Bobdiwala S, Fourie H, Mannino R, Lee Y, Smith A, Marchesi J,  
1100 Timmerman D, Bourne T, Bennett P, MacIntyre D. 2020. The association between  
1101 vaginal bacterial composition and miscarriage: a nested case-control study. *BJOG: An*  
1102 *International Journal of Obstetrics & Gynaecology* 127:264-274.

1103 58. Chan D, Bennett PR, Lee YS, Kundu S, Teoh TG, Adan M, Ahmed S, Brown RG, David  
1104 AL, Lewis HV, Gimeno-Molina B, Norman JE, Stock SJ, Terzidou V, Kropf P, Botto M,  
1105 MacIntyre DA, Sykes L. 2022. Microbial-driven preterm labour involves crosstalk  
1106 between the innate and adaptive immune response. *Nat Commun* 13:975.

1107 59. Miller EA, Beasley DE, Dunn RR, Archie EA. 2016. Lactobacilli Dominance and  
1108 Vaginal pH: Why Is the Human Vaginal Microbiome Unique? *Front Microbiol* 7:1936.

1109 60. Amabebe E, Anumba DOC. 2018. The Vaginal Microenvironment: The Physiologic Role  
1110 of Lactobacilli. *Front Med (Lausanne)* 5:181.

1111 61. Saraf VS, Sheikh SA, Ahmad A, Gillevet PM, Bokhari H, Javed S. 2021. Vaginal  
1112 microbiome: normalcy vs dysbiosis. *Arch Microbiol* doi:10.1007/s00203-021-02414-3.

1113 62. Ravel J, Gajer P, Abdo Z, Schneider GM, Koenig SS, McCulle SL, Karlebach S, Gorle  
1114 R, Russell J, Tacket CO, Brotman RM, Davis CC, Ault K, Peralta L, Forney LJ. 2011.  
1115 Vaginal microbiome of reproductive-age women. *Proc Natl Acad Sci U S A* 108 Suppl  
1116 1:4680-7.

1117 63. Chang DH, Shin J, Rhee MS, Park KR, Cho BK, Lee SK, Kim BC. 2020. Vaginal  
1118 Microbiota Profiles of Native Korean Women and Associations with High-Risk  
1119 Pregnancy. *J Microbiol Biotechnol* 30:248-258.

1120 64. Dunlop AL, Satten GA, Hu YJ, Knight AK, Hill CC, Wright ML, Smith AK, Read TD,  
1121 Pearce BD, Corwin EJ. 2021. Vaginal Microbiome Composition in Early Pregnancy and  
1122 Risk of Spontaneous Preterm and Early Term Birth Among African American Women.  
1123 *Front Cell Infect Microbiol* 11:641005.

1124 65. Kumar S, Kumari N, Talukdar D, Kothidar A, Sarkar M, Mehta O, Kshetrapal P,  
1125 Wadhwa N, Thiruvengadam R, Desiraju BK, Nair GB, Bhatnagar S, Mukherjee S, Das B.  
1126 2021. The Vaginal Microbial Signatures of Preterm Birth Delivery in Indian Women.  
1127 *Front Cell Infect Microbiol* 11:622474.

1128 66. Romero R, Hassan SS, Gajer P, Tarca AL, Fadrosh DW, Nikita L, Galuppi M, Lamont  
1129 RF, Chaemsathong P, Miranda J, Chaiworapongsa T, Ravel J. 2014. The composition  
1130 and stability of the vaginal microbiota of normal pregnant women is different from that of  
1131 non-pregnant women. *Microbiome* 2:4.

1132 67. Han YW, Ikegami A, Bissada NF, Herbst M, Redline RW, Ashmead GG. 2006.  
1133 Transmission of an uncultivated *Bergeyella* strain from the oral cavity to amniotic fluid  
1134 in a case of preterm birth. *J Clin Microbiol* 44:1475-83.

1135 68. Han YW, Fardini Y, Chen C, Iacampo KG, Peraino VA, Shamonki JM, Redline RW.  
1136 2010. Term stillbirth caused by oral *Fusobacterium nucleatum*. *Obstet Gynecol* 115:442-  
1137 5.

1138 69. Davis EP. 1890. TUBERCULOSIS IN PREGNANCY AND PARTURITION.--  
1139 WEBBED FINGER.--DIFFERENTIAL DIAGNOSIS OF PNEUMONIA IN  
1140 CHILDREN.: TUBERCULOSIS IN PREGNANCY AND PARTURITION. WEBBED  
1141 FINGERS. CATARRHAL AND CROUPOUS PNEUMONIA. *Medical and Surgical*  
1142 *Reporter* (1858-1898) 62:420.

1143 70. Huber BM, Meyer Sauteur PM, Unger WWJ, Hasters P, Eugster MR, Brandt S,  
1144 Bloomberg GV, Natalucci G, Berger C. 2018. Vertical Transmission of *Mycoplasma*  
1145 *pneumoniae* Infection. *Neonatology* 114:332-336.

1146 71. Winn HN. 2007. Group B *Streptococcus* Infection in Pregnancy. *Clinics in Perinatology*  
1147 34:387-392.

1148 72. Larsen JW, Sever JL. 2008. Group B *Streptococcus* and pregnancy: a review. *American*  
1149 *Journal of Obstetrics and Gynecology* 198:440-450.

1150 73. Brokaw A, Furuta A, Dacanay M, Rajagopal L, Adams Waldorf KM. 2021. Bacterial and  
1151 Host Determinants of Group B *Streptococcal* Vaginal Colonization and Ascending  
1152 Infection in Pregnancy. *Front Cell Infect Microbiol* 11:720789.

1153 74. Waite DW, Chuvochina M, Pelikan C, Parks DH, Yilmaz P, Wagner M, Loy A,  
1154 Naganuma T, Nakai R, Whitman WB, Hahn MW, Kuever J, Hugenholtz P. 2020.  
1155 Proposal to reclassify the proteobacterial classes *Deltaproteobacteria* and *Oligoflexia*, and  
1156 the phylum *Thermodesulfobacteria* into four phyla reflecting major functional  
1157 capabilities. *International Journal of Systematic and Evolutionary Microbiology* 70:5972-  
1158 6016.

1159 75. Kent WJ. 2002. BLAT - The BLAST-like alignment tool. *Genome Research* 12:656-664.

1160 76. Kanehisa M, Sato Y. 2020. KEGG Mapper for inferring cellular functions from protein  
1161 sequences. *Protein Science* 29:28-35.

1162 77. Seemann T. 2014. Prokka: rapid prokaryotic genome annotation. *Bioinformatics*  
1163 30:2068-9.

1164 78. Madigan MT, Martinko JM, Parker J. 2006. *Brock biology of microorganisms*, vol 11.  
1165 Pearson Prentice Hall Upper Saddle River, NJ.

1166 79. Morris RL, Schmidt TM. 2013. Shallow breathing: bacterial life at low O<sub>2</sub>. *Nature*  
1167 *Reviews Microbiology* 11:205-212.

1168 80. Abusleme L, O'Gorman H, Dutzan N, Greenwell-Wild T, Moutsopoulos NM. 2020.  
1169 Establishment and Stability of the Murine Oral Microbiome. *Journal of Dental Research*  
1170 99:721-729.

1171 81. Rautava J, Pinnell LJ, Vong L, Akseer N, Assa A, Sherman PM. 2015. Oral microbiome  
1172 composition changes in mouse models of colitis. *Journal of Gastroenterology and*  
1173 *Hepatology* 30:521-527.

1174 82. Abusleme L, Hong B-Y, Hoare A, Konkel JE, Diaz PI, Moutsopoulos NM. 2017. Oral  
1175 Microbiome Characterization in Murine Models. *Bio-protocol* 7:e2655.

1176 83. Hernández-Arriaga A, Baumann A, Witte OW, Frahm C, Bergheim I, Camarinha-Silva  
1177 A. 2019. Changes in Oral Microbial Ecology of C57BL/6 Mice at Different Ages  
1178 Associated with Sampling Methodology. *Microorganisms* 7:283.

1179 84. Dickson RP, Erb-Downward JR, Falkowski NR, Hunter EM, Ashley SL, Huffnagle GB.  
1180 2018. The Lung Microbiota of Healthy Mice Are Highly Variable, Cluster by

1181 Environment, and Reflect Variation in Baseline Lung Innate Immunity. American journal  
1182 of respiratory and critical care medicine 198:497-508.

1183 85. Singh N, Vats A, Sharma A, Arora A, Kumar A. 2017. The development of lower  
1184 respiratory tract microbiome in mice. *Microbiome* 5:61-61.

1185 86. Kostric M, Milger K, Krauss-Etschmann S, Engel M, Vestergaard G, Schloter M, Schöler  
1186 A. 2018. Development of a Stable Lung Microbiome in Healthy Neonatal Mice.  
1187 *Microbial Ecology* 75:529-542.

1188 87. Ashley SL, Sjoding MW, Popova AP, Cui TX, Hoostal MJ, Schmidt TM, Branton WR,  
1189 Dieterle MG, Falkowski NR, Baker JM, Hinkle KJ, Konopka KE, Erb-Downward JR,  
1190 Huffnagle GB, Dickson RP. 2020. Lung and gut microbiota are altered by hyperoxia and  
1191 contribute to oxygen-induced lung injury in mice. *Science Translational Medicine*  
1192 12:eaau9959.

1193 88. Poroyko V, Meng F, Meliton A, Afonyushkin T, Ulanov A, Semenyuk E, Latif O, Tesic  
1194 V, Birukova AA, Birukov KG. 2015. Alterations of lung microbiota in a mouse model of  
1195 LPS-induced lung injury. *American journal of physiology Lung cellular and molecular  
1196 physiology* 309:L76-L83.

1197 89. Vrbanac A, Riestra AM, Coady A, Knight R, Nizet V, Patras KA. 2018. The murine  
1198 vaginal microbiota and its perturbation by the human pathogen group B Streptococcus.  
1199 *BMC Microbiology* 18:197.

1200 90. Cowley HM, Heiss GS. 1991. Changes in Vaginal Bacterial Flora During the Oestrous  
1201 Cycle of the Mouse. *Microbial Ecology in Health and Disease* 4:229-235.

1202 91. Noguchi K, Tsukumi K, Urano T. 2003. Qualitative and Quantitative Differences in  
1203 Normal Vaginal Flora of Conventionally Reared Mice, Rats, Hamsters, Rabbits, and  
1204 Dogs. *Comparative Medicine* 53:404-412.

1205 92. Jašarević E, Howard CD, Misic AM, Beiting DP, Bale TL. 2017. Stress during pregnancy  
1206 alters temporal and spatial dynamics of the maternal and offspring microbiome in a sex-  
1207 specific manner. *Scientific Reports* 7:44182.

1208 93. Younge N, McCann JR, Ballard J, Plunkett C, Akhtar S, Araújo-Pérez F, Murtha A,  
1209 Brandon D, Seed PC. 2019. Fetal exposure to the maternal microbiota in humans and  
1210 mice. *JCI Insight* 4.

1211 94. Adhikary S, Nicklas W, Bisgaard M, Boot R, Kuhnert P, Waberschek T, Aalbæk B,  
1212 Korczak B, Christensen H. 2017. Rodentibacter gen. nov. including Rodentibacter  
1213 pneumotropicus comb. nov., Rodentibacter heylii sp. nov., Rodentibacter myodis sp.  
1214 nov., Rodentibacter ratti sp. nov., Rodentibacter heidelbergensis sp. nov., Rodentibacter  
1215 trehalosifermentans sp. nov., Rodentibacter rarus sp. nov., Rodentibacter mrazii and two  
1216 genomospecies. *International Journal of Systematic and Evolutionary Microbiology*  
1217 67:1793-1806.

1218 95. Biggers JD. 1953. The carbohydrate components of the vagina of the normal and  
1219 ovariectomized mouse during oestrogenic stimulation. *Journal of anatomy* 87:327-336.

1220 96. Dal Bello F, Hertel C. 2006. Oral cavity as natural reservoir for intestinal lactobacilli.  
1221 *Systematic and Applied Microbiology* 29:69-76.

1222 97. Ursell LK, Clemente JC, Rideout JR, Gevers D, Caporaso JG, Knight R. 2012. The  
1223 interpersonal and intrapersonal diversity of human-associated microbiota in key body  
1224 sites. *Journal of Allergy and Clinical Immunology* 129:1204-1208.

1225 98. Arumugam M, Raes J, Pelletier E, Le Paslier D, Yamada T, Mende DR, Fernandes GR,  
1226 Tap J, Bruls T, Batto JMM, Bertalan M, Borrue N, Casellas F, Fernandez L, Gautier L,

1227 Hansen T, Hattori M, Hayashi T, Kleerebezem M, Kurokawa K, Leclerc M, Levenez F,  
1228 Manichanh C, Nielsen HB, Nielsen T, Pons N, Poulain J, Qin J, Sicheritz-Ponten T, Tims  
1229 S. 2011. Enterotypes of the human gut microbiome. *Nature* 473.

1230 99. Lozupone CA, Stombaugh JI, Gordon JI, Jansson JK, Knight R. 2012. Diversity, stability  
1231 and resilience of the human gut microbiota. *Nature* 489.

1232 100. Lloyd-Price J, Mahurkar A, Rahnavard G, Crabtree J, Orvis J, Hall AB, Brady A, Creasy  
1233 HH, McCracken C, Giglio MG, McDonald D, Franzosa EA, Knight R, White O,  
1234 Huttenhower C. 2017. Strains, functions and dynamics in the expanded Human  
1235 Microbiome Project. *Nature* 550:61-66.

1236 101. Benga L, Knorr JI, Engelhardt E, Gougoula C, Benten PM, Christensen H, Sager M.  
1237 2019. Current Distribution of Rodentibacter Species Among the Mice and Rats of an  
1238 Experimental Facility. *Journal of the American Association for Laboratory Animal  
1239 Science* 58:475-478.

1240 102. Mirmonsef P, Hotton AL, Gilbert D, Burgad D, Landay A, Weber KM, Cohen M, Ravel  
1241 J, Spear GT. 2014. Free glycogen in vaginal fluids is associated with *Lactobacillus*  
1242 colonization and low vaginal pH. *PLOS ONE* 9:e102467-e102467.

1243 103. Rausch P, Basic M, Batra A, Bischoff SC, Blaut M, Clavel T, Gläsner J, Gopalakrishnan  
1244 S, Grassl GA, Günther C, Haller D, Hirose M, Ibrahim S, Loh G, Mattner J, Nagel S,  
1245 Pabst O, Schmidt F, Siegmund B, Strowig T, Volynets V, Wirtz S, Zeissig S, Zeissig Y,  
1246 Bleich A, Baines JF. 2016. Analysis of factors contributing to variation in the C57BL/6J  
1247 fecal microbiota across German animal facilities. *International Journal of Medical  
1248 Microbiology* 306:343-355.

1249 104. Witjes VM, Boleij A, Halffman W. 2020. Reducing versus Embracing Variation as  
1250 Strategies for Reproducibility: The Microbiome of Laboratory Mice. *Animals* 10:2415.

1251 105. Stevenson BS, Eichorst SA, Wertz JT, Schmidt TM, Breznak JA. 2004. New strategies  
1252 for cultivation and detection of previously uncultured microbes. *Appl Environ Microbiol*  
1253 70:4748-55.

1254 106. Kozich JJ, Westcott SL, Baxter NT, Highlander SK, Schloss PD. 2013. Development of a  
1255 dual-index sequencing strategy and curation pipeline for analyzing amplicon sequence  
1256 data on the MiSeq Illumina sequencing platform. *Appl Environ Microbiol* 79:5112-20.

1257 107. Callahan BJ, McMurdie PJ, Rosen MJ, Han AW, Johnson AJA, Holmes SP. 2016.  
1258 DADA2: High-resolution sample inference from Illumina amplicon data. *Nature Methods*  
1259 13:581-583.

1260 108. Pruesse E, Quast C, Knittel K, Fuchs BM, Ludwig W, Peplies J, Glockner FO. 2007.  
1261 SILVA: a comprehensive online resource for quality checked and aligned ribosomal  
1262 RNA sequence data compatible with ARB. *Nucleic Acids Research* 35:7188-7196.

1263 109. Quast C, Pruesse E, Yilmaz P, Gerken J, Schweer T, Yarza P, Peplies J, Glockner FO.  
1264 2013. The SILVA ribosomal RNA gene database project: improved data processing and  
1265 web-based tools. *Nucleic Acids Res* 41:D590-6.

1266 110. Davis NM, Proctor DM, Holmes SP, Relman DA, Callahan BJ. 2018. Simple statistical  
1267 identification and removal of contaminant sequences in marker-gene and metagenomics  
1268 data. *Microbiome* 6:226.

1269 111. Afgan E, Baker D, Batut B, van den Beek M, Bouvier D, Čech M, Chilton J, Clements D,  
1270 Coraor N, Grüning BA, Guerler A, Hillman-Jackson J, Hiltemann S, Jalili V, Rasche H,  
1271 Soranzo N, Goecks J, Taylor J, Nekrutenko A, Blankenberg D. 2018. The Galaxy

1272 platform for accessible, reproducible and collaborative biomedical analyses: 2018 update.  
1273 Nucleic Acids Research 46:W537-W544.

1274 112. Na S-I, Kim YO, Yoon S-H, Ha S-m, Baek I, Chun J. 2018. UBCG: Up-to-date bacterial  
1275 core gene set and pipeline for phylogenomic tree reconstruction. Journal of Microbiology  
1276 56:280-285.

1277 113. Rambaut A. 2018. FigTree v1.4.4, Institute of Evolutionary Biology, University of  
1278 Edinburgh, Edinburgh. <https://github.com/rambaut/figtree>.

1279 114. Darling ACE, Mau B, Blattner FR, Perna NT. 2004. Mauve: multiple alignment of  
1280 conserved genomic sequence with rearrangements. Genome research 14:1394-1403.

1281 115. Page AJ, Cummins CA, Hunt M, Wong VK, Reuter S, Holden MTG, Fookes M, Falush  
1282 D, Keane JA, Parkhill J. 2015. Roary: rapid large-scale prokaryote pan genome analysis.  
1283 Bioinformatics 31:3691-3693.

1284 116. Tatusova T, DiCuccio M, Badretdin A, Chetvernin V, Nawrocki EP, Zaslavsky L,  
1285 Lomsadze A, Pruitt KD, Borodovsky M, Ostell J. 2016. NCBI prokaryotic genome  
1286 annotation pipeline. Nucleic Acids Research 44:6614-6624.

1287 117. Moriya Y, Itoh M, Okuda S, Yoshizawa AC, Kanehisa M. 2007. KAAS: an automatic  
1288 genome annotation and pathway reconstruction server. Nucleic Acids Res 35:W182-5.

1289 118. Karp PD, Midford PE, Billington R, Kothari A, Krummenacker M, Latendresse M, Ong  
1290 WK, Subhraveti P, Caspi R, Fulcher C, Keseler IM, Paley SM. 2021. Pathway Tools  
1291 version 23.0 update: software for pathway/genome informatics and systems biology.  
1292 Brief Bioinform 22:109-126.

1293 119. Gohir W, Whelan FJ, Surette MG, Moore C, Schertzer JD, Sloboda DM. 2015.  
1294 Pregnancy-related changes in the maternal gut microbiota are dependent upon the  
1295 mother's periconceptional diet. Gut Microbes 6:310-320.

1296 120. Nuriel-Ohayon M, Neuman H, Ziv O, Belogolovski A, Barsheshet Y, Bloch N, Uzan A,  
1297 Lahav R, Peretz A, Frishman S, Hod M, Hadar E, Louzoun Y, Avni O, Koren O. 2019.  
1298 Progesterone Increases Bifidobacterium Relative Abundance during Late Pregnancy. Cell  
1299 Reports 27:730-736.e3.

1300 121. Liu X, Zhang F, Wang Z, Zhang T, Teng C, Wang Z. 2021. Altered gut microbiome  
1301 accompanying with placenta barrier dysfunction programs pregnant complications in  
1302 mice caused by graphene oxide. Ecotoxicology and Environmental Safety 207:111143.

1303